Surgeries on Iterated Torus Knots Bounding Rational Homology 4-Balls

by
Lisa Lokteva

A thesis submitted in fulfillment of the requirements
for the degree of

Doctor of Philosophy

at the

School of Mathematics & Statistics
College of Science & Engineering
University of Glasgow

Contents

List of Figures

List of Appended Papers

This thesis is based on the following papers, which are referred to in the text by their Roman numerals.

I L. Lokteva, *Surgeries on iterated torus knots bounding rational homology 4-balls*. Proceedings of the Edinburgh Mathematical Society, 1-22. (2023) Available from: doi:10.1017/S0013091523000342

II L. Lokteva, *Constructing Rational Homology 3-Spheres That Bound Rational Homology 4-Balls*. Preprint, 2023. Submitted.

Acknowledgements

I would like to express my heartfelt gratitude to all those who have supported me throughout my academic journey, helping me turn my childhood dream of becoming a researcher into reality.

First and foremost, I would like to thank my supervisor Ana Lecuona, who showed me the way into research, taught me everything she knows (well, as much as my head fits), cheered me on during my highest moments, consoled me in my lowest. I will take pride in calling you my academic mother.

Second, I would like to thank Marco Golla, who was not my supervisor, but still gave me so much of his time: guiding me through my questions step-by-step, introducing me to new mathematical topics in long sessions at the blackboard, recommending conferences, receiving me in Nantes when I needed an office to go to, and much more. You may not be my academic father, but definitely my academic cool uncle.

Third, I would like to thank the examiners at my viva: Brendan Owens and Peter Feller; for reading my thesis and providing extremely helpful comments. I am astonished by the amount of mathematics I learnt in the week following my viva, while editing my thesis.

I would also like to thank the institutions and people that hosted me during my PhD. Thanks go to University of Glasgow, that was my sanctuary during these four years. I would especially like to thank Brendan and Mark, who answered so many of my paperwork questions, as well as Tanu, my academic sister, who took her sister job very seriously. Thanks also go to Laboratoire des mathématiques Jean Leray in Nantes and the Alfréd Rényi Institute of Mathematics in Budapest, who received me for two research visits each. Many people from these places deserve special mention. From Nantes, I would like to mention Paolo Ghiggini who so graciously lent me his flat. We did not interact much, but I liked getting to know you through the books and other objects I found in your home. In Budapest, I would first like to thank András Stipsicz, my local host. Thanks for our discussions and for the most amazing course of Heegaard Floer homology ever. I mean it; Heegaard Floer homology seemed so scary before, but now I feel fit for fight. Also from Budapest, I would like to thank Marco Marengon, who upon my arrival welcomed me into the international group with open arms, so that I immediately got a family there. I would also like to thank you for our mathematical discussions, for taking your time to answer my questions and introduce me to new kinds of scary homology theories.

Last but not least as far as institutions go, I would like to thank Montpellier, where I got stuck for 9 months because of the world-wide pandemic in 2020. I cannot complain though. Montpellier was a lovely warm city with lovely warm

people. Thanks go especially to Albin, who woke me up every morning and put me in front of a computer. Everything I did in those 9 months is thanks to you.

In a way, my PhD journey did not start 4 years ago, but at the moment I fell in love with mathematics. I cannot remember when that was, just that I was already hooked on it at the age of 4. Thanks go to Baba Nadya, Deda Sasha and Mama Olya for keeping that interest alive. For the same reason, I would like to thank Valentina Chapovalova for her maths blog and Victor Ufnarovski, former deputy leader of the Swedish IMO team and our coach. Victor, you're like our mathematical grandpa, taking us on trips, telling us mathematical stories, and valiantly defending our solutions.

Finally, I would like to thank my dear friends and lovers, including but not limited to Adrien, Aleksej, Dan, Eki, Losh, Max, Sasha, Signe, and Tanu. If I were to write down all the reasons for me to thank you, that would make another thesis. Thanks for the hugs and the laughs and the madness. I love you.

I wanted to end these acknowledgements with the last paragraph, but I couldn't bear not to give a separate one to Losh. You are the friend of friends, the friendliest of them all. Thanks for your campaign to convert me to university mathematics; for our travels together; for putting up with me crying about exes, cleaning, and paperwork; for your insane presents that commemorate our travels and growing pains, and that I keep as artifacts; for your insane activity ideas that I hate in the moment but make for great stories; for the activities that I love, too; for your multilingual humour; for all your new creative ways to annoy me... Thanks for guiding me through life like you would a little sister. You mean the world to me.

Declaration

I declare that, except where explicit reference is made to the contribution of others, this dissertation is the result of my own work and has not been submitted for any other degree at the University of Glasgow or any other institution.

Chapter 1

Summary and Outline

1.1 Technical Summary

This thesis is on the subject of low-dimensional topology, which studies manifolds of dimensions up to 4. Even more specifically, this thesis lies in the field jokingly called 3.5-dimensional topology, which studies 3-manifolds through the 4-manifolds that they bound. One interesting question in this field is the following:

Question (Casson, [18, Problem 4.5])**.** *Which rational homology* 3*-spheres bound rational homology* 4*-balls?*

In this thesis, we focus our attention on 3-manifolds that are positive surgeries on algebraic knots, a family chosen because of its connection to algebraic geometry. This thesis thus revolves around the following question:

Question. *Which positive surgeries on algebraic knots bound rational homology* 4*-balls?*

This question is studied from different angles in the two papers that this thesis consists of, referred to as [Paper I] and [Paper II]. [Paper I] is focussed entirely on obstructing positive integral surgeries on algebraic knots from bounding rational homology balls. One tool that can be used to obstruct rational homology 3-spheres from bounding rational homology balls is called *lattice embeddings*, but it requires the rational homology sphere in question to have a definite filling in order to be applicable. In [Paper I] we construct such a filling for large enough surgeries on algebraic knots. We use the lattice embedding obstruction on these fillings to obstruct some families of surgeries on algebraic knots from bounding rational homology balls. [Paper II], on the other hand, is more constructive. There, we construct large families of 3-manifolds that we show bound rational homology balls, amongst which we find many examples of rational surgeries on torus knots, the simplest algebraic knots.

1.2 Outline of the Thesis

This thesis is based on two papers, [Paper I] and [Paper II], which are appended in the end, although the online version lacks [Paper I] due to copyright issues. The

purpose of the chapters is to explain how these papers fit into a bigger picture.

To this purpose, Chapter 2, gives an introduction to the field of low-dimensional topology in general and Casson's question for surgeries on algebraic knots in particular. Section 2.1 starts off by introducing the field of low-dimensional topology as well as the intersection forms that lie at the core of 4-manifold theory. The highlight of this section is Donaldson's theorem from 1982, a theorem that revolutionised 4-manifold theory because it allowed us to obstruct the existence of smooth 4-manifolds with certain properties. This was a crucial tool to counterweigh the construction methods of the 70's with which we attempted to construct manifolds whose existence Donaldson proved impossible. What were these construction methods of 4-manifolds? Well, one rich family of examples of 4-manifolds can be obtained from algebraic geometry, namely complex surfaces, but there would be great reason to believe that this is a tiny unrepresentative portion of all 4-manifolds. A much more efficient and general method is by using Kirby diagrams, that is diagrams that give us information on how to glue 4-balls together into a smooth 4-manifold. There is an excellent book [17] that explains all the ins and outs of Kirby calculus, but in Section 2.2 of this thesis, we give a crash course in how to interpret the Kirby diagrams in the appended papers, both as diagrams of 4-manifolds with boundary and as diagrams of the 3-manifolds that bound them. As we go further, we reach Section 2.3, in which we introduce Casson's problem on rational homology 3-spheres bounding rational homology 4-balls. Here, we also introduce the lattice embedding obstruction to a 3-manifold bounding a rational homology 4-ball, an obstruction coming from Donaldson's theorem. Finally, in Section 2.4, we peek into the world of singularity theory in order to explain why it is so interesting to study Casson's question for surgeries on algebraic knots.

While Chapter 2 explains the setting of my research, Chapter 3 summarises my actual results. There is a section for each paper, containing the main results as well as some notes on the techniques used, but the proofs are omitted.

Chapter 2

Background

2.1 Low-Dimensional Topology

Manifolds, spaces that locally look like $\mathbb{R}^n$, have been a major object of mathematical research for over a century. This is not strange, since a major goal of mathematical research is to understand the world, and manifolds regularly occur in nature, not just as descriptions of the physical spaces we live in, but also as all sorts of phase spaces, that is spaces of possible data points.

Manifold theory has been studying the following questions:

Question. *Fix n. Can we make a list of all possible n-manifolds? What properties and structures can they have? (E.g. smooth structures, complex structures, Riemannian metrics, etc.)*

So, what do we know about manifolds? Curves and surfaces, that is manifolds of dimensions 1 and 2, have been well understood since the nineteenth century. They are classified up to homeomorphisms and diffeomorphisms, and their differential geometry is well understood too. Three-manifolds are not classified, but there was steady progress in their study throughout the twentieth century, progress that continues to this day. In the 1960's, high-dimensional topology was revolutionised by the s-cobordism and surgery theorems which were both proved using the so called "Whitney trick". These theorems allowed us to answer many existence and uniqueness questions about manifolds of dimensions ≥ 5 and turned high-dimensional topology into its own subject with quite an algebraic flavour. As for dimension 4, we knew very little until 1981, when Freedman discovered that a version of the Whitney trick could also be applied to 4-manifolds with small enough fundamental group, if we disregard their smooth structures. In fact, this discovery allowed Freedman to classify closed simply connected topological 4-manifolds completely [12]. Almost at the same time, Donaldson used gauge theory to show that smooth 4-manifolds were drastically different from their topological counterparts, and that the Whitney trick fails miserably for them. Four-dimensional manifolds are very interesting in that way, that the topological manifolds and the smooth ones differ so dramatically. A corollary of Freedman's and Donaldson's results is that the topological manifold $\mathbb{R}^4$ has infinitely [16], and in fact uncountably [33, Theorem 1.1], many different smooth structures.

The main character in Freedman's and Donaldson's results is the *intersection form*. A compact, oriented, topological 4-manifold admits a fundamental class

$$[X] \in H_4(X, \partial X; \mathbb{Z})$$

and thus a bilinear form

$$Q_X : H^2(X, \partial X; \mathbb{Z}) \times H^2(X, \partial X; \mathbb{Z}) \to \mathbb{Z}$$

defined by $Q_X(a, b) = \langle a \cup b, [X] \rangle$. Since $a \cup b = (-1)^{2 \cdot 2} b \cup a$, this form is also symmetric. Note that $a \cup b = 0$ if either a or b is torsion, so we can view it as a form on $H^2(X, \partial X; \mathbb{Z})/\text{ Torsion}$. Using Poincaré duality, we can instead view it as a form $H_2(X)/\text{ Torsion} \times H_2(X)/\text{ Torsion} \to \mathbb{Z}$. Fixing a basis of $H_2(X)/\text{ Torsion}$, Q_X can be represented by an integral matrix M. A change of basis can be represented by an integral matrix B of determinant ± 1, and the matrix of Q_X becomes $B^T M B$ under this basis transformation. Thus, $\det(Q_X)$ is well-defined.

If X happens to be a smooth 4-manifold, then every element of $H_2(X; \mathbb{Z})$ can be represented by an embedded surface [17, Proposition 1.2.3.]. This gives us an easy interpretation of Q_X for smooth 4-manifolds. For $a, b \in H^2(X, \partial X; \mathbb{Z})$, let Σ_a, Σ_b be surface representatives of $PD(a), PD(b) \in H_2(X; \mathbb{Z})$. Then the following holds:

Proposition ([17, Proposition 1.2.5])**.** *For $a, b \in H^2(X, \partial X; \mathbb{Z})$, $Q_X(a, b)$ is the number of points in $\Sigma_a \cap \Sigma_b$ counted with sign.*

We can now state Freedman's and Donaldson's theorems:

Theorem (Freedman, [13],[12])**.** *For every symmetric bilinear form $Q : \mathbb{Z}^n \times \mathbb{Z}^n \to \mathbb{Z}$ with $\det(Q) = \pm 1$, there exists a simply connected, closed, topological 4-manifold X such that $Q_X \cong Q$. If Q is even, that is $Q(\alpha, \alpha) \equiv 0 \pmod 2$ for all $\alpha \in \mathbb{Z}^n$, this manifold is unique up to homeomorphism. Otherwise, there are exactly two different homeomorphism types of manifolds with the given intersection form, at most one of which carries a smooth structure.*

Theorem 1 (Donaldson, [8, 9])**.** *If the intersection form Q_X of a smooth, closed 4-manifold X is negative definite, then $Q_X \cong -\operatorname{Id}$.*

Freedman's and Donaldson's theorems were massive breakthroughs in low-dimensional topology because they allowed us to obstruct things in 4-manifold theory. For example, we can show that some topological 4-manifolds have no smooth structure. For example, there exists a closed topological 4-manifolds with this negative definite determinant-1 intersection form:

$$\begin{bmatrix} -2 & 1 & 0 & 0 & 0 & 0 & 0 & 0 \\ 1 & -2 & 1 & 0 & 0 & 0 & 0 & 0 \\ 0 & 1 & -2 & 1 & 0 & 0 & 0 & 0 \\ 0 & 0 & 1 & -2 & 1 & 0 & 0 & 0 \\ 0 & 0 & 0 & 1 & -2 & 1 & 0 & 1 \\ 0 & 0 & 0 & 0 & 1 & -2 & 1 & 0 \\ 0 & 0 & 0 & 0 & 0 & 1 & -2 & 0 \\ 0 & 0 & 0 & 0 & 1 & 0 & 0 & -2 \end{bmatrix},$$

but it cannot have a smooth structure. This thesis heavily uses a corollary to Donaldson's theorem (Theorem 11) to obstruct some 3-manifolds from bounding certain kinds of 4-manifolds, but before talking about that, we will look at some tools to construct 4-manifolds.

2.2 Kirby Diagrams

While 3- and 4-manifolds belong to "low-dimensional" topology, these are still too many dimensions for us humans to be able to visualise with ease. While we may not be able to see 3- and 4-dimensional objects in front of us, we can create diagrams that encode all the relevant information. Kirby diagrams are precisely this kind of tool for drawing 4-manifolds with or without boundary. Morse theory shows that we can construct every compact smooth 4-manifold out of five types of simple building blocks, and a Kirby diagram is a diagram that encodes the gluing information.

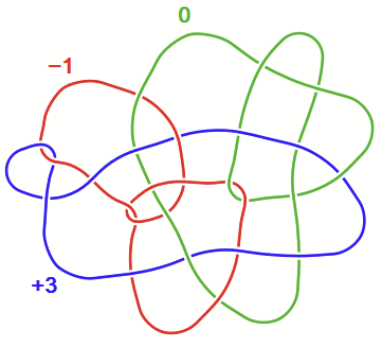

Figure 1: A Kirby diagram representing a 4-manifold with boundary built by attaching three "fat discs" to D^4.

Kirby calculus, the theory of Kirby diagram manipulation, is an essential tool for a low-dimensional topologist that can be learnt in [17, Chapters 4-5]. In this section, we summarise these chapters in order to provide the reader with a crash course in how to interpret the Kirby diagrams and the plumbing/chain graphs in the appended papers.

The purpose of Kirby calculus is to represent 4-manifolds *up to diffeomorphism*. The theory of Kirby calculus consists of the following pieces:

1. **The pieces.** All closed smooth n-manifolds with boundary can be built out of so called n-dimensional handles.

2. **The diagrams.** A Kirby diagram is a diagram that shows how the k-handles are glued together into a 4-manifold.

3. **The calculus.** Two different Kirby diagrams could represent the same 4-manifold up to diffeomorphism. Kirby calculus is to Kirby diagrams what Reidemeister moves are to link diagrams: a sufficient set of diagrammatic operations that take us from one representation of a 4-manifold to any other.

In this section, we will describe the pieces and the diagrams, since they are necessary to understand the results of the thesis, but the calculus is left for the advanced reader to learn in [17].

2.2.1 The Pieces

Definition. For $0 \leq k \leq n$, an n-dimensional k-handle h is a copy of $D^k \times D^{n-k}$ attachable to an n-manifold with boundary X through an embedding $\varphi : \partial D^k \times D^{n-k} \to \partial X$. This attachment is referred to as "adding a k-handle to X".

I like to think of a k-handle as a $D^k \times D^{n-k}$ with boundary $(\partial D^k \times D^{n-k}) \cup (D^k \times \partial D^{n-k})$, with glue on the $\partial D^k \times D^{n-k}$ bit and no glue on the $D^k \times \partial D^{n-k}$ bit.

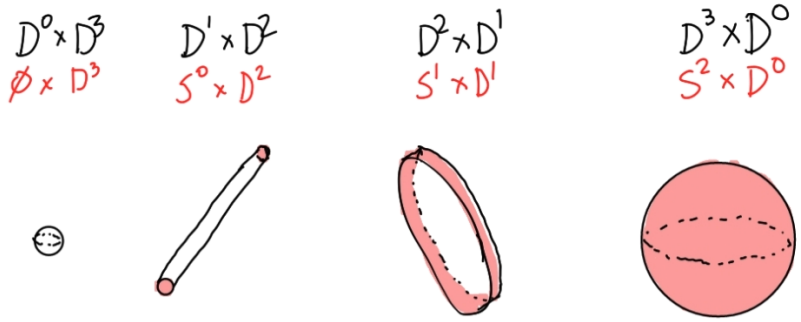

Figure 2: 3-dimensional handles. The glue is shown in red.

When attaching a k-handle, there is a canonical way to smooth corners, so attaching a handle to a smooth manifold gives us a new smooth manifold of the same dimension. Also note that $X \cup_\varphi h$ deformation retracts onto $X \cup_{\varphi|_{\partial D^k \times \{0\}}} D^k \times \{0\}$, so up to homotopy, attaching a k-handle amounts to attaching a k-cell. Thus we can also think of an n-dimensional k-handle as a k-cell that has been thickened to an n-dimensional object.

2.2.2 The Diagrams

From Morse theory, we get the following theorem:

Theorem ([32, Theorem D])**.** *Every closed connected smooth manifold has a self-indexing Morse function with exactly one minimum and one maximum.*

This theorem has a very important corollary:

Corollary 2. *All closed connected smooth n-manifolds M can be built by attaching handles the following way:*

(0) *Attach a 0-handle to empty space to create the manifold $X_0 = D^n$.*

(1) *Attach a number of 1-handles to X_0 to create a manifold X_1.*

$(i+1)$ *Attach a number of* $(i+1)$*-handles to* X_i *to create a manifold* X_{i+1}*.*

(n) *Attach one* n*-handle to create the closed manifold* $X_n \cong M$*.*

Thus, if we want to build a closed 4-manifold, we start by attaching n 1-handles to D^4 along the boundary, and obtain $\natural^n S^1 \times D^3$. Thereafter, we attach some 2-handles. Now, the boundary of X_2 should be the same as the boundary of the union of the 3- and 4-handles, which should, by symmetry, be $\natural^n S^1 \times D^3$. As it happens, there is a unique way up to diffeomorphism to glue $\natural^n S^1 \times D^3$ into $\partial(\natural^n S^1 \times D^3) = \#^n S^1 \times S^2$, so in order to specify the closed 4-manifold, we only need to explain the gluing of the 1- and 2-handles. This is exactly the information that a Kirby diagram contains.

In this thesis on 3.5-dimensional topology, we do not use any 1-handles. This is because 3.5-dimensional topologists usually only need 2-handles, for reasons given in Subsection 2.2.4. We will thus only explain how to read Kirby diagrams with 2-handles only.

A 4-manifold with boundary X_2 consisting of one 0-handle and s 2-handles is of the form $D^4 \cup_{(\varphi_1,\dots,\varphi_s)} \bigsqcup_{i=1}^s (D^2 \times D^2)$, where $\varphi_i : (S^1 \times D^2) \to \partial D^4$ are embeddings with disjoint images. Since we only want to specify X_2 up to diffeomorphism, it is enough to specify $\varphi := \bigsqcup_{i=1}^s \varphi_i$ up to isotopy. What information can we scale away?

The first thing we note is that the image of φ is a disjoint union of solid tori embedded in S^3. Composing φ with a self-isotopy of S^3 will yield a 2-handle attachment map giving the same 4-manifold. This roughly says that isotopies of the image of φ do not matter for the diffeomorphism class of X_2.

The second thing we need to ask ourselves is if knowing the image of φ_i is enough to specify φ_i up to isotopy. The answer is no, because there is a free and transitive action of $\mathbb{Z}$ on the isotopy classes of diffeomorphisms $\psi : S^1 \times D^2 \to S^1 \times D^2$, where n acts as the postcomposition with the self-diffeomorphism $f_n(e^{i\theta_1}, re^{i\theta_2}) = (e^{i\theta_1}, re^{i\theta_2} e^{in\theta_1})$. Thus, the isotopy classes of diffeomorphisms between two different solid tori can be described using an integer, as long as we can choose a particular diffeomorphism to be labelled 0.

Taking the above considerations into account, [17, Chapters 4-5] show that we can describe φ_i up to isotopy with the following two data points:

1. the knot $K = \varphi_i(S^1 \times \{0\})$ (and thereby its tubular neighbourhood, which is isotopic to $\varphi_i(S^1 \times D^2)$), and
2. an integer $n := \mathrm{lk}(K, \varphi_i(S^1 \times \{p\}))$ for $0 \neq p \in D^2$, called the **framing**.

Thus, a typical Kirby diagram in this thesis is a link where each component is assigned an integer, as in Figure 1.

2.2.3 A Trinity of Kirby Diagram Interpretations

So far, we have been talking about Kirby diagrams as representations of connected closed smooth 4-manifolds. Every connected closed smooth 4-manifold can be represented by a Kirby diagram, possibly using 1-handles. However, not every Kirby diagram we can think of represents a *closed* smooth manifold. If we draw an

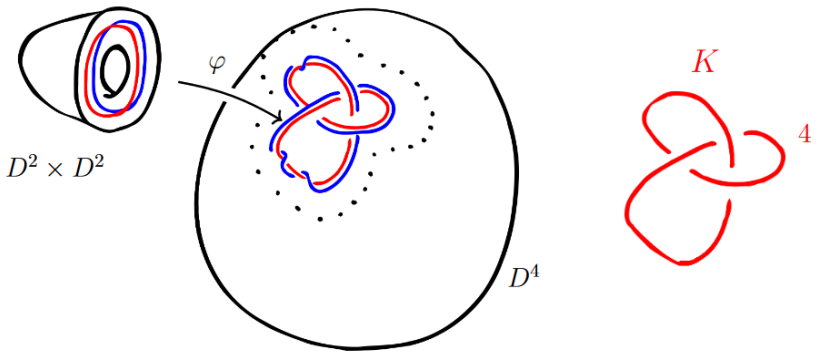

Figure 3: The meaning of a knot with a number. The linking number of the red and the blue knots is 4.

integer-weighted link, we can construct a manifold with boundary X_2 by attaching 2-handles according to the diagram information. However, unless $\partial X_2 \cong S^3$, we will not be able to close the manifold by attaching a 4-handle. However, we can still use that Kirby diagram as a simultaneous representation of the manifold with boundary X_2 and the 3-manifold ∂X_2. In fact, it is these two interpretations that are most useful in 3.5-dimensional topology.

To summarise, these are the possible interpretations of a Kirby diagram:

1. Just adding 1-handles and 2-handles to D^4 according to the data specified in the Kirby diagram gives us some 4-manifold with boundary X_2. Not all 4-manifolds with boundary can be described using such a diagram with no 3- or 4-handles.

2. The boundary of X_2 is some closed 3-manifold, so we can say that the Kirby diagram is a description of the 3-manifold ∂X_2. Every closed orientable connected 3-manifold can be described using a Kirby diagram with nothing but 2-handles (see Corollary 5).

3. If $\partial X_2 \cong \natural_n S^1 \times D^3$, then we can in a unique way add 3- and 4-handles to X to obtain a closed 4-manifold. Every smooth closed oriented connected 4-manifold can be described by this kind of Kirby diagram (possibly with 1-handles).

Each of these interpretations of Kirby diagrams have their own set of operations that preserve the diffeomorphism class of the manifold described. These operations, the Kirby diagram analogues of Reidemeister moves for link diagrams, can be found in [17, Chapters 4-5].

2.2.4 Dehn/Rational Surgery

We have just seen how we can describe 3-manifolds using Kirby diagrams, by viewing them as the boundary of some 4-manifold with boundary. This section is all about forgetting about the 4-manifold with boundary and viewing our weighted link simply as the diagram of a 3-manifold.

Question. *What does each 2-handle attachment do to ∂X_2?*

Answer. Recall that the boundary of a 4-dimensional 2-handle $D^2 \times D^2$ is $(S^1 \times D^2) \cup (D^2 \times S^1)$, the first component covered in glue. When we attach a 2-handle to a 4-manifold, the boundary 3-manifold changes through the removal of a solid torus and the gluing of a different one in along the boundary, which is a torus.

How do we describe this gluing? Well, we can describe it by saying where the meridian $S^1 \times \{1\}$ of new solid torus $D^2 \times S^1$ goes. For that we need a definition:

Definition. Let $K \subset S^3$ be an oriented smooth knot. The boundary $\partial(\nu K)$ of a tubular neighbourhood νK of K is an embedded torus in S^3. The **meridian** M and the **longitude** L are oriented simple closed curves inside $\partial(\nu K)$, determined up to isotopy by the following homology and linking relations:

- $[M] = 0$ and $[L] = [K]$ in $H_1(\nu K)$, and
- $\mathrm{lk}(M, K) = 1$ and $\mathrm{lk}(L, K) = 0$.

So, say that we have some 4-manifold X with boundary Y and we attach a 2-handle $D^2 \times D^2$ through a map $\varphi : S^1 \times D^2 \to S^3$. Recall that up to diffeomorphism of the resulting manifold, the map φ can be described just by the knot $K = \varphi(S^1 \times \{0\})$ and $n = \mathrm{lk}(K, \varphi(S^1 \times \{1\}))$. What happens to the boundary is that we take out $\varphi(S^1 \times D^2)$, which is a tubular neighbourhood of K, and glue a new solid torus along the boundary into the hole $\varphi(S^1 \times S^1) = \partial \nu K$, in such a way that $\varphi(S^1 \times \{1\})$ becomes the new meridian. This new meridian can, up to isotopy, be described by the homology class $[L] + n[M] \in H_1(\partial(\nu K))$. □

Now we know that the 3-manifold represented by a Kirby diagram

$$(K_1, n_1; \ldots; K_s, n_s)$$

with no 1-handles is S^3 but with the tubular neighbourhoods of the knots K_i replaced by a different solid torus, whose meridian is a curve in homology class $[L_i] + n_i[M_i] \in H_1(\partial(\nu K_i))$. However, if we want to use Kirby diagrams as descriptions of 3-manifolds only, no 4-manifolds, there is no reason why we couldn't generalise them to say "Take out a tubular neighbourhood of K and glue in a solid torus so that it obtains meridian $q[L]+p[M] \in H_1(\partial(\nu K))$." Such generalised Kirby diagrams are called **surgery diagrams**.

Definition (Dehn/Rational surgery)**.** Let p and q be relatively prime integers. A p/q-**surgery** on K inside S^3, denoted $S^3_{\frac{p}{q}}(K)$ is the manifold $(S^3 - \nu K) \cup_\varphi D^2 \times S^1$, where the diffeomorphism $\varphi : \partial S^1 \times S^1 \to \partial \nu K$ is such that $[\varphi(S^1 \times \{1\})] = q[L] + p[M] \in H_1(\partial(\nu K))$. The case of $p = \pm 1$ and $q = 0$ is called an ∞-surgery and $S^3_\infty(K) \cong S^3$.

Proposition 3. *Dehn surgery is a well-defined operation on oriented smooth manifolds up to oriented diffeomorphism.*

Definition. A **surgery diagram** is a diagram of a link L in S^3 where each component K_i is assigned a rational number r_i. It represents a 3-manifold obtained from performing an r_i-surgery on each K_i.

Note that a surgery diagram with only integral weights can be viewed as a Kirby diagram, and this view gives the *same* 3-*manifold*. While a surgery diagram with rational weights does not come with a 4-dimensional filling, a surgery diagram with only integral ones automatically does.

What is cool though is that *every rational surgery diagram can be replaced by an integral surgery diagram representing the same* 3-*manifold*. This can be done using the **slam-dunk** move [17, p. 163]. It is illustrated in Figure 4.

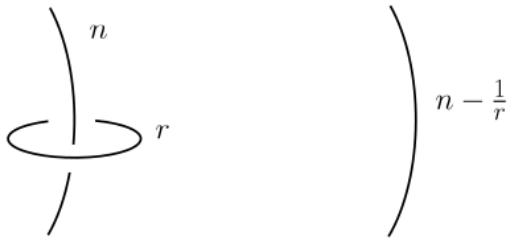

Figure 4: This operation on surgery diagrams, called the slam-dunk, does not change the represented 3-manifold. Here the segment is a portion of a knot K, the closed loop is necessarily a meridian of K, $n \in \mathbb{Z}$ and $r \in \mathbb{Q} \cup \{\infty\}$.

So, if component K_i of the link in the surgery diagram has surgery coefficient $\frac{p_i}{q_i}$ and

$$\frac{p_i}{q_i} = a_1 - \cfrac{1}{a_2 - \cfrac{1}{\ddots - \cfrac{1}{a_n.}}} =: [a_1, a_2, \ldots, a_n]^-$$

for some integer values $a_1, \ldots, a_n$, then we can attach a "chain" of length $n-1$ to K_i and give both K_i and the new chain components the integer coefficients $a_1, a_2, \ldots, a_n$ in order, as in Figure 5.

We finish this section by showing that every closed orientable connected 3-manifold has a 4-dimensional filling. We will first need the following black box of a theorem:

Theorem 4 (Lickorish-Wallace Theorem, 60's, [35, Theorem 6], [22, Theorem 2])**.** *Every closed orientable connected* 3*-manifold can be obtained as a Dehn surgery on some* $\mathbb{Q}$*-weighted link in* S^3*.*

Now we can use the fact that we can replace any surgery diagram by an integral surgery diagram to obtain:

Corollary 5 (Proven directly in [22, proof of Theorem 2, p. 539])**.** *Every closed connected orientable* 3*-manifold can be represented by a Kirby diagram with nothing but* 2*-handles.*

But, since every Kirby diagram represents both a 3-manifold and a 4-manifold with said 3-manifold for a boundary, we get:

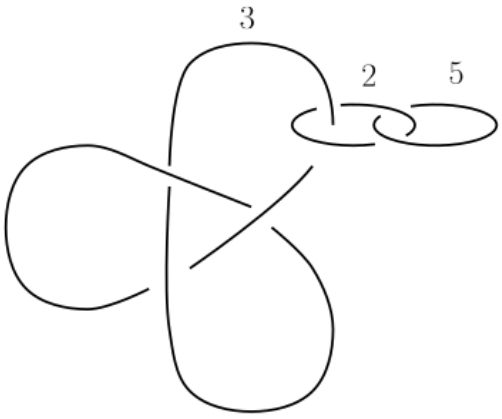

Figure 5: This is an integral surgery diagram of $S^3_{\frac{22}{9}}(K)$ where K is the right-handed trefoil. This diagram is obtained by writing $\frac{22}{9} = [3, 2, 5]^-$ and using the reverse slam-dunk move to expand the chain from K.

Corollary 6 ([22, Theorem 3])**.** *Every closed connected orientable* 3*-manifold is the boundary of some simply-connected* 4*-manifold with boundary.*

Note that the fact that every 3-manifold is the boundary of a 4-manifold was known much earlier, for instance to Rohlin in 1951 [28], but the above sequence of corollaries might be more useful to a 3.5-dimensional topologist wanting to find a filling for their 3-manifolds constructed by surgery.

2.2.5 Intersection Forms

One of the main points of Kirby diagrams is that they allow us to construct smooth 3- and 4-manifolds with all sorts of desired properties. For example, given any symmetric bilinear form $Q : \mathbb{Z}^n \times \mathbb{Z}^n \to \mathbb{Z}$, we can construct a simply connected smooth 4-manifold *with boundary* with that intersection form.

How, you may ask? Well, given a 4-manifold with boundary X_2 (or closed 4-manifold X) described by a Kirby diagram with only 2-handles, what is its intersection form?

Proposition 7. *Consider a Kirby diagram consisting of an* n*-component link* $L = \bigsqcup_{i=1}^n K_i$ *with weights* $\vec{w} = (w_1, \ldots, w_n)$*. Then the described* 4*-manifold* X_2 *has* $H_2(X_2) = \mathbb{Z}(S_1, \ldots, S_n)$*, for* S_i *the union of the core* $D^2 \times \{0\}$ *of the* 2*-handle attached along* K_i *and the cone on* K_i *inside the* 0*-handle* D^4*. In this basis,* X_2 *has the intersection form*

$$Q_X(S_i, S_j) = \begin{cases} w_i & \text{if } i = j \\ \mathrm{lk}(K_i, K_j) & \text{if } i \neq j. \end{cases}$$

Now, given a symmetric bilinear form, it is not hard to draw some link with matching linking numbers. In fact, there as at least as many ways to do that as

there are knots. For example, given the matrix

$$\begin{pmatrix} 6 & -2 & -3 \\ -2 & -2 & 3 \\ -3 & 3 & -1 \end{pmatrix},$$

we can draw both the Kirby diagram in Figure 6 and the Kirby diagram in Figure 7. (However, nothing a priori prevents these diagrams from representing the same 4-manifold.)

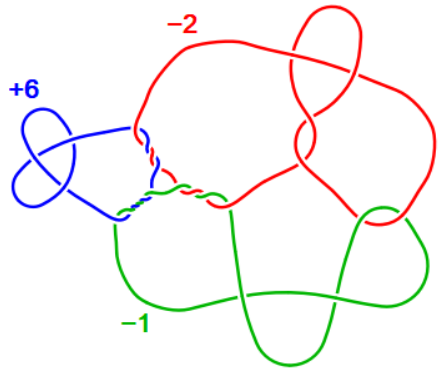

Figure 6: A complicated Kirby diagram with a simple intersection form.

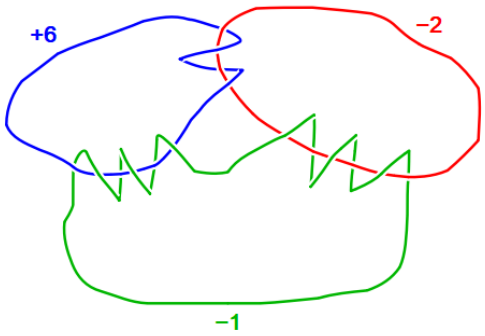

Figure 7: A simple Kirby diagram with the same intersection form.

Corollary 8. *For any symmetric bilinear form $Q : \mathbb{Z}^n \times \mathbb{Z}^n \to \mathbb{Z}$, there exists a simply connected smooth 4-manifold with boundary with that intersection form.*

2.2.6 Special Kirby Diagrams

In the appended papers, the Kirby diagrams that appear are especially simple. One of the simple families of 4-manifolds we consider are those whose Kirby diagram consists of just one knot K and its framing/weight n. In [Paper I, Section 3], we denote such a 4-manifold with boundary by $D^4_n(K)$. Its boundary is denoted $S^3_n(K)$.

The other simple family of 4-manifolds with boundary that appears in this thesis is the family of plumbings described by weighted forests. While plumbed 4-manifolds are usually defined as being constructed out of disc bundles over surfaces (see [17, Section 6.1]), the following alternative definition is enough for the purposes of this thesis:

Definition. Given a forest-shaped plumbing graph Γ with weight function $W : V \to \mathbb{Z}$, we may associate to it a 4-manifold X_Γ by describing its Kirby diagram. First, we draw a small unknot at each vertex of Γ. Then, for each edge, we create a Hopf linking between the knots corresponding to the edge ends as in Figure 8. We denote the resulting link by L_Γ. Then X_Γ is the simply-connected 4-manifold obtained by attaching 2-handles with framing $W(v)$ to the unknot at each vertex v.

We denote the 3-manifold ∂X_Γ by Y_Γ.

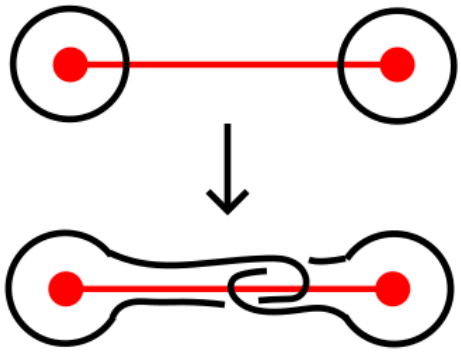

Figure 8: Kirby diagram associated to a plumbing.

2.3 Casson's Problem

We have now seen that every closed orientable 3-manifold Y is the boundary of some simply-connected 4-manifold X. (We say that X is a **filling** of Y.) While this is in itself a really impressive and interesting result, we can explore it even further. If we introduce some conditions on Y, can we find a filling X with additional properties? The field of study of the interactions between 3-manifolds and their 4-dimensional fillings is tongue-in-cheek called "3.5-dimensional topology".

This thesis is concerned with the study of rational homology spheres and rational homology balls. These are 3- and 4-dimensional objects that through the eyes of one algebraic invariant look like 3-dimensional spheres and 4-dimensional balls, respectively.

Definition. For a manifold M, we say that a manifold N is a **rational homology** M if M and N are of the same dimension and $H_*(M;\mathbb{Q}) \cong H_*(N;\mathbb{Q})$.

Remark. Note that all rational homology n-balls (B^n) have the same homology. When the dimension of the manifold N is clear, we might just refer to N as a "rational homology ball" without specifying the dimension.

This thesis is concerned with the following problem, attributed to Casson, which appears as Problem 4.5 on Kirby's list of the most important problems in low-dimensional topology [18].

Question 9 (Casson)**.** *Which rational homology* 3*-spheres (*$\mathbb{QH}S^3$*s) bound rational homology* 4*-balls (*$\mathbb{QH}B^4$*s)?*

Rational homology 3-spheres abound in nature. For example, $Y = S^3_{p/q}(K)$, the p/q-surgery on K, satisfies $H_1(Y) = \mathbb{Z}/p\mathbb{Z}$ for all knots K and non-zero rational numbers p/q. However, very few of them bound rational homology balls, as shown by [2, Theorem 1.1]:

Theorem 10 (Aceto-Golla)**.** *For a given knot K and integer $q \neq 0$, there exist at most* 4 *values of p such that $S^3_{\frac{p}{q}}(K) = \partial\mathbb{QH}B^4$.*

The two most common methods for obstructing 3-manifolds from bounding rational homology balls are lattice embeddings and Heegaard Floer correction terms. Aceto and Golla used Heegaard Floer correction terms to prove their theorem. Lattice embeddings is a technique that was first systematically used by Paolo Lisca in [23]. It is based on the following corollary to Donaldson's Theorem [8], in this thesis referred to as Theorem 1:

Theorem 11 (Corollary of Donaldson's Theorem)**.** *Let Y be a rational homology 3-sphere and $Y = \partial X$ for X a negative definite smooth connected oriented 4-manifold. If $Y = \partial W$ for a smooth rational homology 4-ball W, then there exists a lattice embedding*

$$f : (H_2(X)/\operatorname{Torsion}, Q_X) \hookrightarrow (\mathbb{Z}^{\operatorname{rk} H_2(X)}, -\operatorname{Id}),$$

i.e. a map $f : H_2(X)/\operatorname{Torsion} \to \mathbb{Z}^{\operatorname{rk} H_2(X)}$ such that $Q_X(a,b) = -f(a)\cdot f(b)$, where $\cdot$ is the Euclidean dot product.

Imagine now that I have a rational homology 3-sphere Y and I want to show that it does not bound a rational homology ball. In order to use the lattice embedding obstruction, I need to first find a definite X such that $Y = \partial X$. This is not necessarily easy and such an X might not even exist [14, 27, 15]. Suppose it does exist and that we have found its intersection form. Now, it is easy to check if a lattice embedding exists. Let $\{e_i\}_{1\leq i\leq \operatorname{rk} H_2(X)}$ be a basis of $\mathbb{Z}^{\operatorname{rk} H_2(X)}$. Every basis vector v of $H_2(X)/\operatorname{Torsion}$ has to map to $\sum_{i=1}^{\operatorname{rk} H_2(X)} \lambda_i e_i$ where $|\sum_{i=1}^{\operatorname{rk} H_2(X)} \lambda_i^2| = |Q_X(v,v)|$, which leaves us with finitely many possible images for each basis vector. We might find out that a lattice embedding actually does exist. In that case, there might exist a different definite filling X' of Y for which there does not. All the more challenging is checking this obstruction for a whole family of 3-manifolds Y at once. This difficulty is described in the introduction of Paper II.

The first study of rational homology 3-spheres bounding rational homology 4-balls was published in 1981, when Casson and Harer found several families of homology lens spaces bounding rational homology 4-balls and homology 3-spheres

bounding contractible manifolds [6]. In 2007, Lisca classified all the so called lens spaces (rational surgeries on the unknot) and connected sums of lens spaces bounding rational homology 4-balls [23, 24], popularising the technique of obstructing bounding rational homology 4-balls with lattice embeddings. Many people have since then used lattice embeddings on various classes of 3-manifolds to classify the ones that admit fillings with certain homological constraints. Examples include Lecuona's study of double branched covers of S^3 branched over some families of Montesinos knots [21], Aceto's study of rational homology $S^1 \times S^2$s bounding rational homology $S^1 \times D^3$s [1], and Simone's classifying torus bundles on the circle bounding rational homology $S^1 \times D^3$s [30], which he used to construct rational homology 3-spheres bounding rational homology 4-balls in [31]. Recently, Aceto, Golla, Larson and Lecuona managed to answer Casson's question for positive integral surgeries on positive torus knots, a classification with a whopping 18 cases [2, 3].

This thesis studies Casson's question for surgeries on so called algebraic knots, which is a class of knots arising in singularity theory. Both the unknot and all positive torus knots are algebraic knots, so one can view my question as a natural continuation of the work done in [23, 2, 3]. In order to define algebraic knots, we will however take a little tour through the algebraic geometry and topology of singular algebraic plane curves.

2.4 Algebraic Knots and Rational Cuspidal Curves

Let's leave the realm of topology for a while for something completely different. We are instead going to dive into the world of algebraic curves in $\mathbb{C}P^2$. Algebraic curves are possibly singular surfaces inside $\mathbb{C}P^2$ that arise as solutions to polynomial equations and are a classical object of study for algebraic geometers. In this section, we are going to introduce the reader to the question of classifying singular algebraic curves, and then explain its complicated relationship to Casson's question.

Readers who wish to delve deeper beyond this brief introduction would benefit from exploring [5] and [34], both of which are standard texts on algebraic plane curves. However, the author learned this material from a topological book, namely [10], which explores invariants of graph manifolds, with singularities of plane algebraic curves as its central motivating example.

Definition. An **affine plane curve** is the zero set inside $\mathbb{C}^2$ of a non-zero polynomial $f \in \mathbb{C}[x, y]$. It is denoted by $V(f)$.

Definition. A **projective plane curve** is the zero set inside $\mathbb{C}P^2$ of some non-zero homogeneous polynomial $F \in \mathbb{C}[x, y, z]$. It is denoted by $V(F)$.

We call both affine and projective plane curves **(complex) algebraic**, just to set them apart from smooth curves in $\mathbb{R}^2$. Note that algebraic curves are 2-real-dimensional.

Already now, we can formulate the most fundamental question of algebraic plane curves:

Question 12. *What can an algebraic plane curve look like?*

This question is not very precise. We can ask what object this solution set looks like topologically, that is up to homeomorphism. We can also ask about how this topological object is embedded in $\mathbb{C}^2$ or $\mathbb{C}P^2$. We can also ask about the holomorphic structure of the curve. For now, we want to study Question 12 topologically, that is up to homeomorphism and maybe diffeomorphism.

First, let's look at some examples of algebraic curves. In Figure 9, we see three polynomials together with their real solution sets. Since we only have the real picture in front of us, we cannot see the shape of the surfaces that the solution sets form. We do however see that they cannot always be manifolds, since they might have singularities. In Figure 9b, there is a self-intersection, and in Figure 9c, there is a cusp.

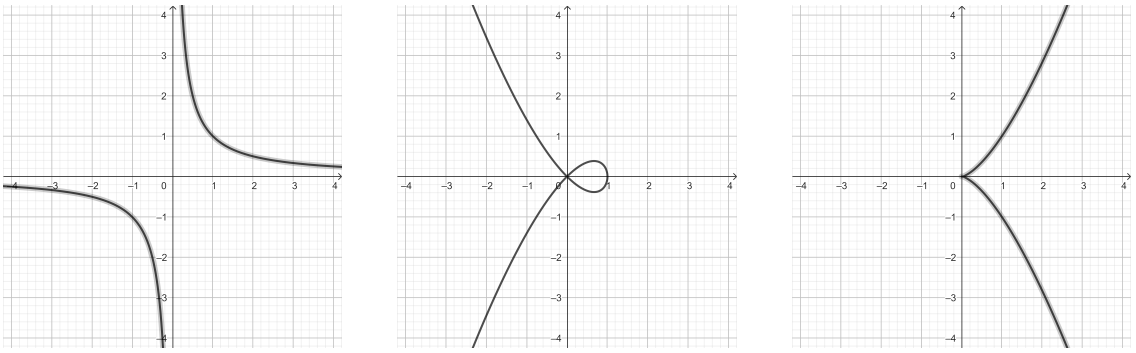

(a) $xy - 1 = 0$ (b) $-x^3 + x^2 - y^2 = 0$ (c) $y^2 - x^3 = 0$

Figure 9: Examples of algebraic curves.

Definition. A **singular point** of an affine plane curve is a point $p = (p_1, p_2) \in V(f)$ such that $\left(\frac{\partial f}{\partial x}, \frac{\partial f}{\partial y}\right)|_p = (0, 0)$.

Recall that the projective plane is covered by the affine charts $[x : y : 1]$, $[x : 1 : z]$ and $[1 : y : z]$, so we can study local properties inside affine charts. A point on a projective curve is singular if it is singular inside an affine chart.

A curve without singular points is called **non-singular**, and is notoriously boring topologically. Non-singular projective plane curves are 2-dimensional submanifolds of $\mathbb{C}P^2$. Their genus is directly dependent on the degree of the polynomial (see for example [19, Chapter 4] for multiple proofs of this standard result):

$$g = \frac{(d-1)(d-2)}{2},$$

and moreover, two non-singular projective curves of the same degree are always isotopic to each other (due to the variety of singular projective curves, a.k.a. *the discriminant locus*, having real codimension 2 inside the moduli space of all projective curves). Let us instead focus on singular curves.

We start by focussing on the local topology of a singularity.

Question 13. *What does a singularity of an algebraic curve look like?*

In other words, if an algebraic curve is not locally homeomorphic to the pair $(\mathbb{R}^4, \mathbb{R}^2)$, what does it actually look like around a singularity? One good answer comes from considering singularity links.

Theorem 14 ([25, Theorem 2.10])**.** *Let $f \in \mathbb{C}[x, y]$ be a non-zero polynomial vanishing at 0. Also let $C = V(f) = \{(x, y) \in \mathbb{C}^2 \mid f(x, y) = 0\}$. For small enough ε, the pair $(D^4_\varepsilon, C \cap D^4_\varepsilon)$ is homeomorphic to the pair consisting of the cone on S^3_ε and the cone on $C \cap S^3_\varepsilon$. Here D^4_ε and S^3_ε are a 4-ball and a 3-sphere, respectively, of radius ε centred at 0.*

Definition. The link $C \cap S^3_\varepsilon \subset S^3$ is called the **singularity link** of C at 0.

Theorem 14 shows the singularity link completely describes the topological type of the singularity. The cone on one link component is a topological disc, but, unless the link is the unknot, this disc can be embedded into D^4 in an interesting way. If the singularity link has only one component, we call the singularity **cuspidal**. If the singularity link consists of several components, this means that the singularity is an intersection of multiple branches (as in Figure 9b), which might or might not themselves be weird cusps (as when $(y^2 - x^3)(y^2 + x^3) = 0$). A knot that is the link of some cuspidal singularity is called **algebraic**.

Example 15. The curve in Figure 9a is non-singular. A non-singular point always has the unknot as its singularity link. The curve in Figure 9b has a transversal intersection of two smooth components at 0, which corresponds to the singularity link being the Hopf link. The singularity at 0 of the curve in Figure 9c is more interesting. This singularity is cuspidal. Its singularity link is the right-handed trefoil knot $T(2, 3)$.

So, can we classify all the possible singularity links? In fact, we can. Both [10, Appendix to Chapter 1], [5, pp. 431-439], and [34, Section 5.4] describe different ways to translate the algebraic data of a singularity (Puiseux or Newton pairs) into the topological data of a singularity link. In particular, they show that all algebraic knots are in fact **iterated torus knots**, which we now define:

Definition. Let p, q be relatively prime integers, and K a knot in S^3. We denote by $C_{p,q}(K) \subset S^3$, the unique (up to isotopy) simple closed curve in $\partial(\nu K)$ with homology class $p[L] + q[M] \in H_1(\partial(\nu K))$. The curve $\mathbb{C}_{p,q}(K)$ is called the (p, q)-**cable** on K.

Definition. The **iterated torus knot** with k iterations $T(p_1, \alpha_1; p_2, \alpha_2; \cdots ; p_k, \alpha_k)$ is the knot

$$T(p_1, \alpha_1; p_2, \alpha_2; \cdots ; p_k, \alpha_k) = C_{p_k,\alpha_k} C_{p_{k-1},\alpha_{k-1}} \cdots C_{p_1,\alpha_1}(O),$$

O being the unknot.

Theorem 16 (Immediate corollary to [10, Proposition 1A.1])**.** *A knot is algebraic if and only if it is an iterated torus knot*

$$T(p_1, \alpha_1; \cdots ; p_k, \alpha_k)$$

satisfying

- *that* $p_i, \alpha_i \geq 2$ *for all* $1 \leq i \leq k$, *and*
- *that* $\alpha_{i+1} > p_{i+1}p_i\alpha_i$ *for all* $1 \leq i \leq k-1$.

A projective plane curve with only cuspidal singularities (no self-intersections) is called **cuspidal**. Theorem 16 answers the local question for cuspidal curves, that is what a cuspidal curve looks like at a singularity. However, we would also want to know what the curve looks like globally. Some relevant statistics we would like to know are

1. the entire collection of local singularity types, and
2. the genus of the curve.

It is not known if these data points determine the curve up to isotopy or homeomorphism of the complement. This certainly is false for line arrangements in $\mathbb{C}P^2$ [29]. However, this data does determine the topology of the tubular neighbourhood of the curve.

Definition. An algebraic plane curve C is called **rational** if it is birational to $\mathbb{C}P^1$.

For a topologist, this implies that there is a diffeomorphism from $C - P$ to $\mathbb{C}P^1 - Q$ for $P \subset C$ and $Q \subset \mathbb{C}P^1$ finite sets of points. Since $CP^1 \cong S^2$, this means that C is some sort of singular sphere, possibly with self-intersections. If C is also cuspidal, it is truly a topological sphere.

The following is a a restricted version of the question of what a singular curve looks like globally:

Question 17. *What are the possible collections of singularities of a rational cuspidal curve?*

We can even restrict it further:

Question 18. *Let* K *be an algebraic knot. Can it be the link of an only singularity of a rational cuspidal curve?*

A projective curve with only one singularity, which is also cuspidal, is called **unicuspidal**.

These questions have been studied by algebraic geometers and low-dimensional topologists alike. The reason for the low-dimensional topologists' interest is the following:

Proposition 19. *Let* $C \subset \mathbb{C}P^2$ *be a rational cuspidal curve of degree* d *with singularity links* $(K_1, \ldots, K_l)$. *Then* νC *is the* 4*-manifold obtained by attaching a* d^2*-framed* 2*-handle along* $K_1 \# \cdots \# K_l$, $\partial \nu C \cong S^3_{d^2}(K_1 \# \cdots \# K_l)$, *and* $\mathbb{C}P^2 - \nu C$ *is a rational homology ball.*

We invite the reader onto a rollercoaster of thoughts on this proposition's significance:

1. If K is an algebraic knot and $S^3_{d^2}(K)$ does not bound a rational homology ball, then there is no rational unicuspidal curve of degree d whose only singularity has link K. We can therefore consider the following weaking of Question 18:

   Question 20. *For which algebraic knots K and integers d does $S^3_{d^2}(K)$ bound a rational homology ball?*

   Us topologists, we have a few tools to obstruct $S^3_{d^2}(K)$ from bounding rational homology balls. Maybe we could help the algebraic geometers to answer Question 18? Unfortunately, obstructing $S^3_{d^2}(K)$ from bounding rational homology balls seems harder than obstructing rational unicuspidal curves of degree d from having singularity link K. For example, [11] told us in 2007 when a torus knot is the only singularity link of a rational cuspidal curve, but it took until 2020 for [3] to tell us when $S^3_{d^2}(T(p,q))$ bounds a rational homology ball. In the meantime, [4] managed to answer Question 18 for cables on torus knots too, whereas [Paper I] from 2023 is the best that we currently have for the corresponding topological question.

2. Maybe the algebraic geometers can help us topologists instead? After all, they often do by providing us with examples. Here too, we can find many examples of $S^3_{d^2}(K)$ bounding rational homology balls in papers like [11] and [4]. Can we find examples not coming from algebraic geometry? Comparing the results of [11] (listing the torus knots that occur as singularity links of unicuspidal curves) and [3] (listing the positive torus knots that admit a positive integral surgery that bounds a rational homology 4-ball) tells us that we can, that is $S^3_{d^2}(K)$ bounding a rational homology ball is more permissive than the existence of a rational unicuspidal curve of degree d with singularity link K. We conclude that while algebraic geometry provides us with nice first examples, the purely topological Casson question for surgeries on singularity links is strictly more supple than Question 18. This probably doesn't surprise anyone. However, it is often still interesting to compare algebro-geometric and topological results and measure how different they are and why. A great result in that vein, proven by Kronheimer and Mrowka in [20], but better known as *the Thom conjecture*, states that smooth algebraic curves are the minimal genus representatives of their homology classes in $\mathbb{C}P^2$, so while there exist many more smooth surfaces than algebraic curves embedded in $\mathbb{C}P^2$, the algebraic ones are in some sense the best.

3. While Questions 18 and 20 are quite different with the former being more rigid and the latter more supple, Question 20 is not entirely disconnected from algebraic geometry. Algebraic geometry is good for constructing 4-manifolds and sometimes we need to construct something in order to obstruct something else. In [Paper I, Section 3], we use the fact that the knots considered are algebraic in order to construct negative definite fillings of $S^3_{d^2}(K)$ on which we can use Theorem 11 to obstruct $S^3_{d^2}(K)$ from bounding rational homology balls.

Chapter 3

On the Appended Papers

Both appended papers are on the theme of Casson's question, that is "Which rational homology 3-spheres bound rational homology 4-balls?" The studied rational homology 3-spheres are positive surgeries on algebraic knots. However, Paper I is an obstructive paper, whereas Paper II is constructive.

In this chapter, we summarise the results of the papers, and give a few comments on their history and the choice of methodology.

3.1 Paper I

The main objective of Paper I is to use lattice embeddings to obstruct integral surgeries on algebraic knots from bounding rational homology balls.

A prerequisite for using lattice embeddings to obstruct a rational homology ball from filling a 3-manifold Y is having a definite filling of Y. In [Paper I, Section 3], we use blow-up resolutions of singularities to construct negative definite fillings for all 3-manifolds $Y = S^3_n(K)$ where K is an algebraic knot and n is large enough.

Theorem 21 (Paper I, Theorem 8)**.** *Let $K = T(p_1, \alpha_1; p_2, \alpha_2; \dots; p_k, \alpha_k)$ be an algebraic knot and let $n \geq p_k\alpha_k + 2$. Then $S^3_n(K)$ bounds a negative definite plumbed 4-manifold with the graph shown in Figure 10, where each hook W_i is described by Figure 11. Here, $N = n - p_k\alpha_k$, $[c_{i,2}, c_{i,3}, \dots, c_{i,s_i}]^- = \frac{\alpha_i}{\alpha_i - p_i}$ and $[d_{i,1}, d_{i,2}, \dots, d_{i,t_i}]^- = \frac{\alpha_i}{p_i}$.*

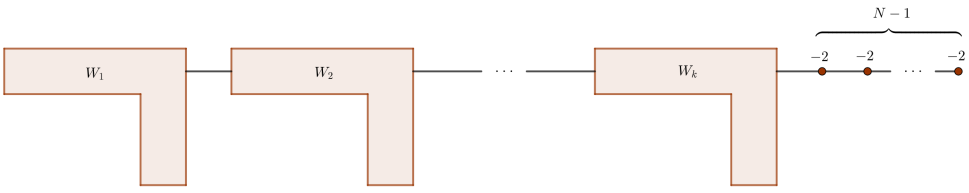

Figure 10: The minimal negative definite plumbing diagram of $S^3_n(T(p_1, \alpha_1; p_2, \alpha_2; \dots; p_k, \alpha_k))$. Each W_i is a subgraph described by Figure 11. Here $N = n - p_k\alpha_k$.

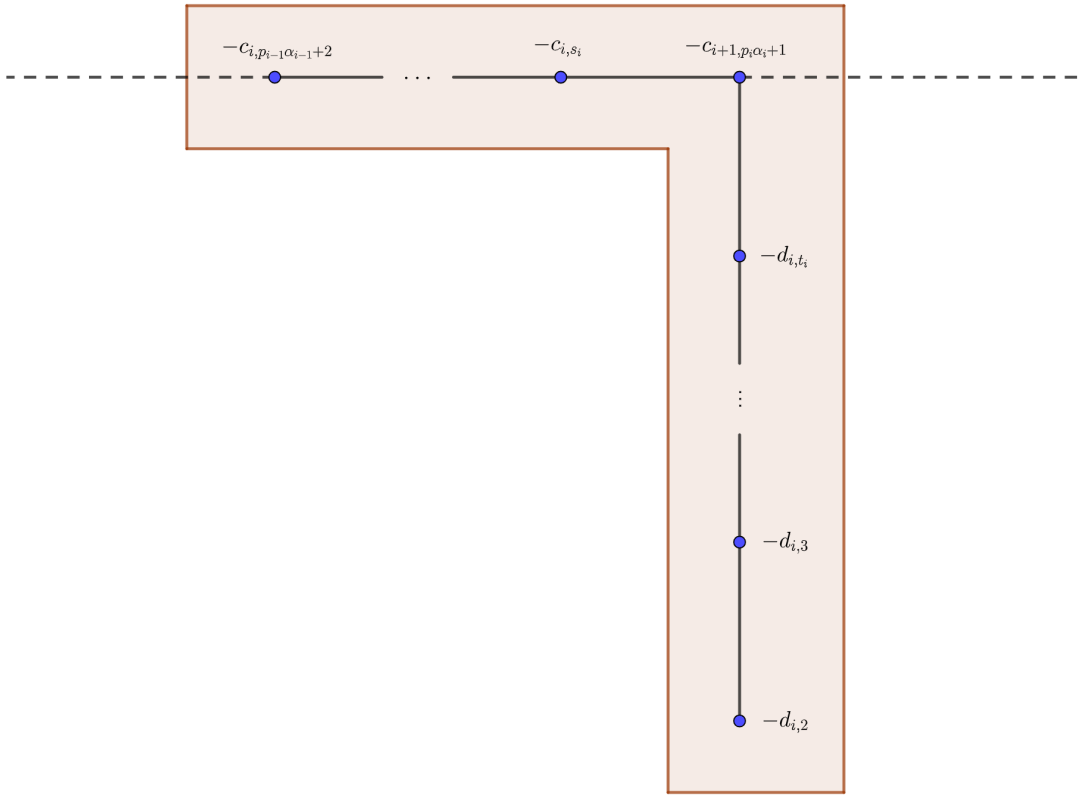

Figure 11: Close-up diagram of each W_i part of the plumbing diagram of $S^3_n(T(p_1,\alpha_1;p_2,\alpha_2;\ldots;p_k,\alpha_k))$ in Figure 10. In order for this diagram to make sense at the extremities, interpret $p_0\alpha_0$ as 0, and $-c_{k+1,p_k\alpha_k+1}$ as -2.

Thereafter, in [Paper I, Section 4], we use the lattice obstruction of Theorem 11 to show:

Theorem 22 (Paper I, Theorem 2)**.** *Let* $\alpha_1 \equiv 1 \pmod{p_1}$, $\alpha_2 \equiv \pm 1 \pmod{p_2}$, $\alpha_2/p_2 > p_1\alpha_1$ *and* $n \geq 2+p_2\alpha_2$. *Then the rational homology* 3*-sphere* $S^3_n(T(p_1,\alpha_1;p_2,\alpha_2))$ *bounds a rational homology* 4*-ball if and only if the tuple* $(p_1,\alpha_1;p_2,\alpha_2;n)$ *is one of the following:*

1. $(p_1, p_1+1; p_2, p_2(p_1+1)^2-1; p_2^2(p_1+1)^2)$ *or*
2. $(2, 7; p_2, 16p_2-1; 16p_2^2)$.

The condition $\alpha_2/p_2 > p_1\alpha_1$ is equivalent to demanding that $T(p_1,\alpha_1;p_2,\alpha_2)$ be algebraic. This condition, together with $n \geq 2+p_2\alpha_2$ are necessary in order to be able to use Theorem 21 to obtain a negative definite filling of $S^3_n(T(p_1,\alpha_1;p_2,\alpha_2))$ to perform a lattice analysis on. The other two conditions, however, are there to simplify the lattice embedding analysis.

Recall, that while testing for a lattice embedding obstruction on one 3-manifold Y with a negative definite filling X is easy, this can be extremely difficult to do for an infinite family at once. People that work with lattice embeddings know some tricks for this. One trick, used by for example [23, 24, 21, 3], requires that $Y = \partial X$,

where $X = X_\Gamma$ for a chain graph Γ, such that $-\operatorname{tr} Q_X - 3\dim H_2(X) \leq -1$, and such that removing one vertex from Γ gives us something whose lattice embeddings have already been classified. Unfortunately, these conditions are only satisfied for $S^3_n(T(p_1, \alpha_1; p_2, \alpha_2))$ when $\alpha_2 = 1 + p_2 + p_1\alpha_1 p_2$. Under this restriction on α_2, the trick helps with the lattice embedding analysis, but still does not completely solve the problem of which $S^3_n(T(p_1, \alpha_1; p_2, 1 + p_2 + p_1\alpha_1 p_2))$ bound a rational homology ball.

Instead, we have, analogously to [2], assumed that $\alpha_1 \equiv 1 \pmod{p_1}$ and $\alpha_2 \equiv \pm 1 \pmod{p_2}$. This makes sure that the weights of the graph in Figure 10 are nearly all -2. Chains of -2 have very few possible embeddings and the possible embeddings of the vertices with other weights are constrained by some Diophantine equations, which we solve.

3.2 Paper II

Paper II naturally sprung out of my project of studying which $S^3_n(T(p_1, \alpha_1; p_2, 1 + p_2 + p_1\alpha_1 p_2))$ bound a rational homology ball. Just like the event of a manifold $S^3_n(K)$ bounding a rational homology ball, the event of the intersection lattice of a negative definite filling of $S^3_n(K)$ admitting a lattice embedding happens very rarely. This makes you wonder: what does an intersection lattice special enough to be embeddable look like?

Studying the tree-shaped chain graphs Γ for which $(H_2(X_\Gamma), Q_{X_\Gamma})$ admits a lattice embedding revealed some patterns. Very often, they looked like some famously lattice embeddable small graph with a couple of so called "complementary legs" grown on top.

Definition. Two sequences $(a_1, a_2, \ldots, a_m)$ and $(b_1, b_2, \ldots, b_n)$ with $a_i, b_j \geq 2$ are **complementary** if and only if $1/[a_1, \ldots, a_m]^- + 1/[b_1, \ldots, b_n]^- = 1$.

Definition. A **pair of complementary legs** is a union of two path graphs with weights $(-a_1, -a_2, \ldots, -a_m)$ and $(-b_1, -b_2, \ldots, -b_n)$, respectively, such that the sequences $(a_1, a_2, \ldots, a_m)$ and $(b_1, b_2, \ldots, b_n)$ are complementary.

In [Paper II, Section 2], we recall some basic facts about complementary legs and their lattice embeddings.

In [Paper II, Section 3], we define what it means to grow complementary legs. This is done through defining two operations (called GOCL and IGOCL moves, standing for *(inner) growth of complementary legs*) on chain graphs with lattice embeddings. The operations preserve lattice embeddability, so growing complementary legs on an enbeddable graph gives us another embeddable graph. However, the existence of an embedding of the intersection lattice of X_Γ does not imply that ∂X_Γ bounds a rational homology ball. The main result of [Paper II, Section 3] is that ∂X_Γ does in fact bound a rational homology ball when Γ is obtained from the famously lattice embeddable [23, 21] $(-3, -2, -2, -3)$- or $(-3, -2, -3, -3, -3)$-weighted path graphs through applying GOCL and IGOCL moves. Figures 12 and 13 show the results of these operations.

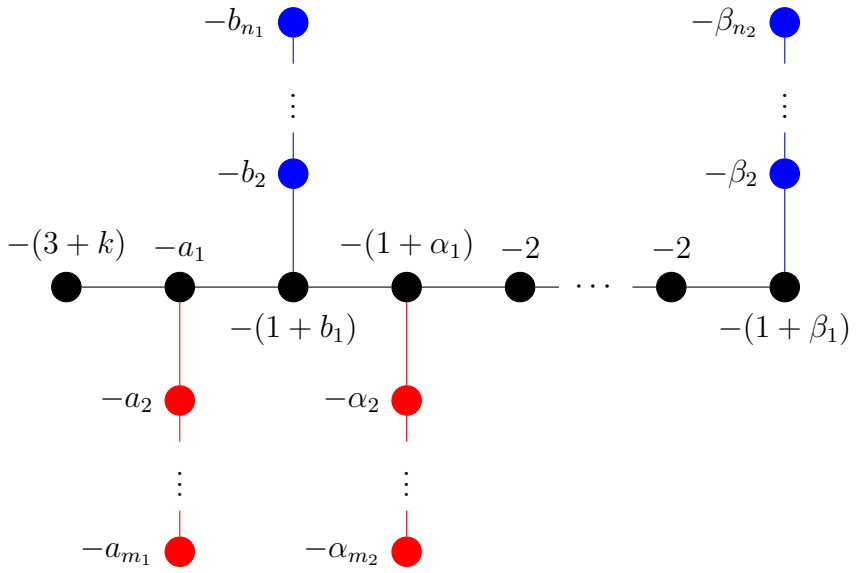

Figure 12: These are the graphs obtainable by performing IGOCL and GOCL moves on the linear graph $(-3,-2,-3,-3,-3)$. Here the length of the chain of -2's is $k \geq 0$, $(a_1,\ldots,a_{m_1})$ and $(\alpha_1,\ldots,\alpha_{m_2})$ are complementary sequences, and $(b_1,\ldots,b_{n_1})$ and $(\beta_1,\ldots,\beta_{n_2})$ are complementary sequences.

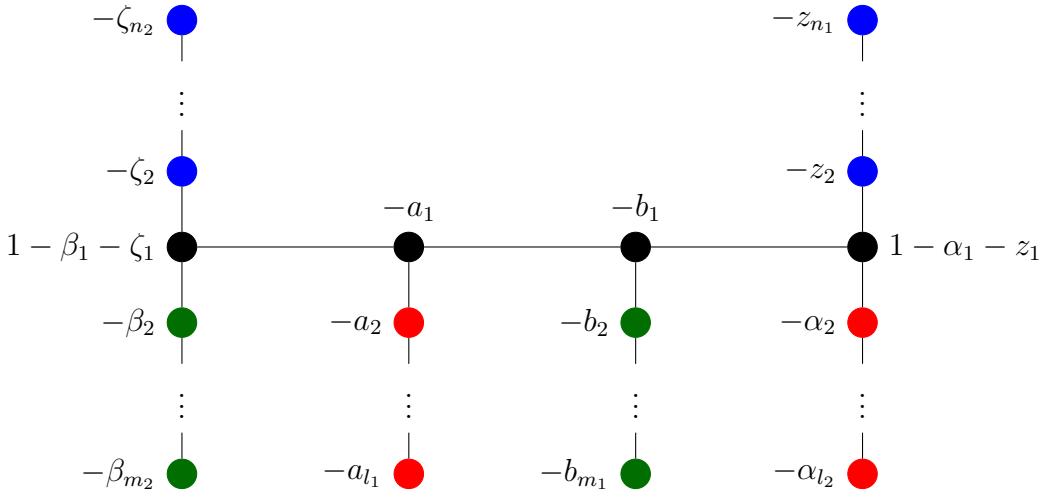

Figure 13: The form of all graphs obtainable from $(-3,-2,-2,-3)$ using GOCL moves. Here the sequences $(a_1,\ldots,a_{l_1})$ and $(\alpha_1,\ldots,\alpha_{l_2})$ are complementary, as well as the sequences $(b_1,\ldots,b_{m_1})$ and $(\beta_1,\ldots,\beta_{m_2})$, and the sequences $(z_1,\ldots,z_{n_1})$ and $(\zeta_1,\ldots,\zeta_{n_2})$.

Theorem 23. *All 3-manifolds described by the chain graphs in Figures 12 and 13 bound rational homology balls.*

Sketch of proof. In this proof we use strongly invertible links:

Definition. A **strongly invertible link** is a link $L \subset \mathbb{R}^3$ such that

1. it is invariant under 180° rotation around the x-axis, and
2. every component intersects the x-axis in exactly two points.

In [26], Montesinos shows that a 4-manifold constructed by attaching 2-handles along a strongly invertible link is the double cover of D^4 branched over a surface that he describes. This is how we use this knowledge:

1. Let Γ be one of the graphs in Figure 12 or 13. The Kirby diagram of a tree-shaped chain graph is always strongly invertible. Representing it in such a way allows us to describe X_Γ as the double branched cover D^4 branched over some surface S_Γ.
2. We show that we can add one or two 2-handles to the $\mathbb{Z}/2\mathbb{Z}$-equivariant Kirby diagram of X_Γ in such a way that the attaching link stays strongly invertible, and such that this new 4-manifold X' happens to be $S^1 \times S^2$ or $(S^1 \times S^2)\#(S^1 \times S^2)$ respectively. It follows that X' is the double cover of D^4 branched over a surface S' that has two or three boundary components respectively, which are unknotted and unlinked in S^3. From the construction, we have that S' is just S_Γ with one or two bands attached, respectively. These band attachments provide us with a cobordism from ∂S_Γ to either the two- or three-component unlink.
3. The fact that $\partial S'$ is an unlink in S^3 means that we can cap it off with discs in D^4. The union of these two or three disks with the one or two bands we attached to turn ∂S_Γ into $\partial S'$ is a surface S of Euler characteristic 1.
4. We use [7, Proposition 2.6] which says that the double branched cover of D^4 over a surface of Euler characteristic 1 is a rational homology ball to show that ∂X_Γ is the boundary of the rational homology ball $\Sigma(D^4, S)$.

□

Another short famously embeddable path graph is $(-2, -2, -3, -4)$. It is missing from the current version of [Paper II]. While we believe that all graphs obtainable from it using GOCL and IGOCL moves do bound rational homology balls, we are unable to prove it using the method described above since we cannot find a way to perform step 2, that is to equivariantly add two -1-weighted 2-handles and obtain $(S^1 \times S^2)\#(S^1 \times S^2)$. We cannot seem to prove that all the graphs in Figure 14 bound a rational homology ball. For a subset of these, we can make do with one -1-weighted 2-handle only, in which case we can find a good rational homology ball filling of the boundary.

In [Paper II, Section 4], we find interesting subsets of the graphs of Figures 12 and 13, namely ones that describe 3-manifolds that are rational surgeries on torus

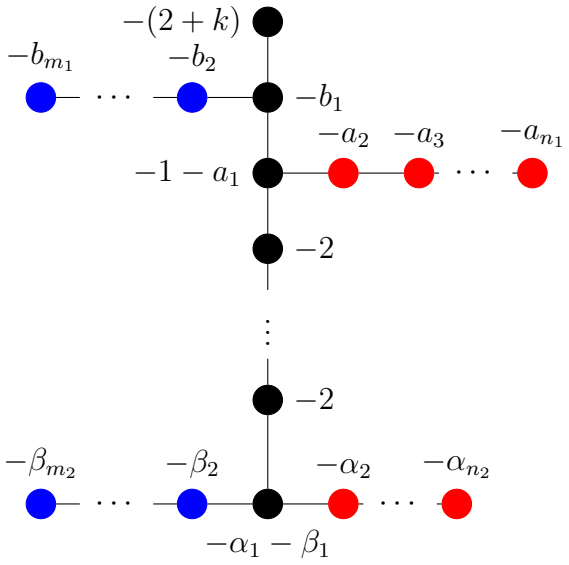

Figure 14: Graphs obtainable from the path graph $(-2,-2,-3,-4)$ using GOCL and IGOCL moves. Here the sequences $(a_1,\dots,a_{n_1})$ and $(\alpha_1,\dots,\alpha_{n_2})$ are complementary, and the sequences $(b_1,\dots,b_{m_1})$ and $(\beta_1,\dots,\beta_{m_2})$ are complementary as well. The length of the chain of -2's is k.

knots. We show the following theorem, which provides us with new, previously unknown, examples of rational surgeries on iterated torus knots bounding rational homology balls.

Theorem 24. *For the following pairs (p,q) with $1<p<q$ and $\mathrm{GCD}(p,q)=1$, there is at least one $r\in\mathbb{Q}_+$ such that $S^3_r(T(p,q))$ bounds a rational ball. Here $k,l\geq 0$.*

1. $(k+2,(l+1)(k+2)+1)$
2. $(k+2,(l+2)(k+2)-1)$
3. $(2k+3,(l+1)(2k+3)+2)$
4. $(2k+3,(l+2)(2k+3)-2)$
5. $(k^2+7k+11,k^3+12k^2+45k+51)$
6. $(S^{(k)}_{l+1},S^{(k)}_{l+2})$ *for* $(S^{(k)}_i)$ *a sequence defined by* $S^{(k)}_0=1$, $S^{(k)}_1=2$, $S^{(k)}_2=2k+7$ *and* $S^{(k)}_{i+2}=(k+4)S^{(k)}_{i+1}-S^{(k)}_i$.
7. $(T^{(k)}_{l+1},T^{(k)}_{l+2})$ *for* $(T^{(k)}_i)$ *a sequence defined by* $T^{(k)}_0=1$, $T^{(k)}_1=k+2$, $T^{(k)}_2=k^2+6k+7$ *and* $T^{(k)}_{i+2}=(k+4)T^{(k)}_{i+1}-T^{(k)}_i$.
8. (U_{l+1},U_{l+2}) *for* (U_i) *a sequence defined by* $U_0=1$, $U_1=3$, $U_2=14$ *and* $U_{i+2}=5U_{i+1}-U_i$.

Assuming that all graph of Figure 14 bound rational homology balls, we can conjecturally extend the list with these items:

1. (P_{l+1}, P_{l+2}) for (P_i) a sequence defined by $P_0 = 1$, $P_1 = 4$, $P_2 = 19$ and $P_{i+2} = 5P_{i+1} - P_i$.

2. (Q_{l+1}, Q_{l+2}) for (Q_i) a sequence defined by $Q_0 = 1$, $Q_1 = 2$, $Q_2 = 9$ and $Q_{i+2} = 5Q_{i+1} - Q_i$.

Currently, however, it is unknown if these bound rational homology balls.

Bibliography

[1] Paolo Aceto. "Rational homology cobordisms of plumbed manifolds". In: *Algebr. Geom. Topol.* 20.3 (2020), pp. 1073–1126. ISSN: 1472-2747. DOI: 10.2140/agt.2020.20.1073.

[2] Paolo Aceto and Marco Golla. "Dehn surgeries and rational homology balls". In: *Algebr. Geom. Topol.* 17.1 (2017), pp. 487–527. ISSN: 1472-2747. DOI: 10.2140/agt.2017.17.487.

[3] Paolo Aceto, Marco Golla, Kyle Larson and Ana G. Lecuona. "Surgeries on torus knots, rational balls, and cabling". In: *arXiv e-prints*, arXiv:2008.06760 (Aug. 2020), arXiv:2008.06760. arXiv: 2008.06760 [math.GT].

[4] J. Bodnár. "Classification of rational unicuspidal curves with two Newton pairs". In: *Acta Math. Hungar.* 148.2 (2016), pp. 294–299. ISSN: 0236-5294.

[5] Egbert Brieskorn and Horst Knörrer. *Plane algebraic curves*. Translated from the German by John Stillwell. Birkhäuser Verlag, Basel, 1986, pp. vi+721. ISBN: 3-7643-1769-8. DOI: 10.1007/978-3-0348-5097-1. URL: https://doi.org/10.1007/978-3-0348-5097-1.

[6] Andrew J. Casson and John L. Harer. "Some homology lens spaces which bound rational homology balls". In: *Pacific J. Math.* 96.1 (1981), pp. 23–36. ISSN: 0030-8730.

[7] Andrew Donald and Brendan Owens. "Concordance groups of links". In: *Algebr. Geom. Topol.* 12.4 (2012), pp. 2069–2093. ISSN: 1472-2747.

[8] S. K. Donaldson. "An application of gauge theory to four dimensional topology". In: *J. Differential Geom.* 18.2 (1983), pp. 279–315. ISSN: 0022-040X.

[9] S. K. Donaldson. "The orientation of Yang-Mills moduli spaces and 4-manifold topology". In: *Journal of Differential Geometry* 26.3 (1987), pp. 397–428. DOI: 10.4310/jdg/1214441485. URL: https://doi.org/10.4310/jdg/1214441485.

[10] David Eisenbud and Walter Neumann. *Three-dimensional link theory and invariants of plane curve singularities*. Vol. 110. Annals of Mathematics Studies. Princeton University Press, Princeton, NJ, 1985, pp. vii+173. ISBN: 0-691-08380-0; 0-691-08381-9.

[11] Javier Fernández de Bobadilla, Ignacio Luengo, Alejandro Melle Hernández and Andras Némethi. "Classification of rational unicuspidal projective curves whose singularities have one Puiseux pair". In: *Real and complex singularities*. Trends Math. Birkhäuser, Basel, 2007, pp. 31–45. DOI: 10.1007/978-3-7643-7776-2_4.

[12] Michael H. Freedman and Frank Quinn. *Topology of 4-manifolds*. Vol. 39. Princeton Mathematical Series. Princeton University Press, Princeton, NJ, 1990, pp. viii+259. ISBN: 0-691-08577-3.

[13] Michael Hartley Freedman. "The topology of four-dimensional manifolds". In: *J. Differential Geometry* 17.3 (1982), pp. 357–453. ISSN: 0022-040X.

[14] Kim A. Frøyshov. *Mod 2 instanton homology and 4-manifolds with boundary*. 2023. arXiv: 2307.03950 [math.GT].

[15] Marco Golla and Kyle Larson. *3-manifolds that bound no definite 4-manifold*. 2020. DOI: 10.48550/ARXIV.2012.12929. URL: https://arxiv.org/abs/2012.12929.

[16] Robert E. Gompf. "An infinite set of exotic $\mathbf{R}^4$'s". In: *Journal of Differential Geometry* 21 (1985), pp. 283–300. URL: https://api.semanticscholar.org/CorpusID:117928223.

[17] Robert E. Gompf and András I. Stipsicz. 4-*manifolds and Kirby calculus*. Vol. 20. Graduate Studies in Mathematics. American Mathematical Society, Providence, RI, 1999, pp. xvi+558. ISBN: 0-8218-0994-6.

[18] Rob Kirby. "Problems in low-dimensional topology". In: *Geometric topology*. AMS/IP Stud. Adv.Math., vol. 2. Amer. Math. Soc., Providence, R.I., 1997, pp. 35–473.

[19] Frances Kirwan. *Complex Algebraic Curves*. London Mathematical Society Student Texts. Cambridge University Press, 1992. DOI: 10.1017/CBO9780511623929.

[20] P. B. Kronheimer and T. S. Mrowka. "The genus of embedded surfaces in the projective plane". In: *Math. Res. Lett.* 1.6 (1994), pp. 797–808. ISSN: 1073-2780.

[21] Ana G. Lecuona. "On the slice-ribbon conjecture for Montesinos knots". In: *Trans. Amer. Math. Soc.* 364.1 (2012), pp. 233–285. ISSN: 0002-9947.

[22] W. B. R. Lickorish. "A Representation of Orientable Combinatorial 3-Manifolds". In: *Annals of Mathematics* 76.3 (1962), pp. 531–540. ISSN: 0003486X. URL: http://www.jstor.org/stable/1970373 (visited on 04/07/2023).

[23] Paolo Lisca. "Lens spaces, rational balls and the ribbon conjecture". In: *Geom. Topol.* 11 (2007), pp. 429–472. ISSN: 1465-3060.

[24] Paolo Lisca. "Sums of lens spaces bounding rational balls". In: *Algebr. Geom. Topol.* 7 (2007), pp. 2141–2164. ISSN: 1472-2747.

[25] J.W. Milnor. *Singular Points of Complex Hypersurfaces*. Annals of mathematics studies. Princeton University Press, 1968. ISBN: 9780691080659.

[26] José María Montesinos. "4-manifolds, 3-fold covering spaces and ribbons". In: *Trans. Amer. Math. Soc.* 245 (1978), pp. 453–467. ISSN: 0002-9947.

[27] Yuta Nozaki, Kouki Sato and Masaki Taniguchi. *Filtered instanton Floer homology and the homology cobordism group*. 2022. arXiv: 1905.04001 [math.GT].

[28] V. A. Rohlin. "A three-dimensional manifold is the boundary of a four-dimensional one". In: *Doklady Akad. Nauk SSSR (N.S.)* 81 (1951), pp. 355–357.

[29] G. L. Rybnikov. "On the fundamental group of the complement of a complex hyperplane arrangement". In: *Funktsional. Anal. i Prilozhen.* 45.2 (2011), pp. 71–85. ISSN: 0374-1990,2305-2899.

[30] Jonathan Simone. "Classification of torus bundles that bound rational homology circles". In: *arXiv preprint arXiv:2006.14986* (2020).

[31] Jonathan Simone. "Using rational homology circles to construct rational homology balls". In: *Topology and its Applications* 291 (2021), p. 107626.

[32] Stephen Smale. "Generalized Poincaré's conjecture in dimensions greater than four". In: *Ann. of Math. (2)* 74 (1961), pp. 391–406. ISSN: 0003-486X.

[33] Clifford Henry Taubes. "Gauge theory on asymptotically periodic 4-manifolds". In: *Journal of Differential Geometry* 25.3 (1987), pp. 363–430. DOI: 10.4310/jdg/1214440981. URL: https://doi.org/10.4310/jdg/1214440981.

[34] C. T. C. Wall. *Singular points of plane curves*. Vol. 63. London Mathematical Society Student Texts. Cambridge University Press, Cambridge, 2004, pp. xii+370. ISBN: 0-521-83904-1; 0-521-54774-1. DOI: 10.1017/CBO9780511617560.

[35] Andrew H. Wallace. "Modifications and cobounding manifolds". In: *Canadian J. Math.* 12 (1960), pp. 503–528. ISSN: 0008-414X,1496-4279. DOI: 10.4153/CJM-1960-045-7. URL: https://doi.org/10.4153/CJM-1960-045-7.

Paper I

SURGERIES ON ITERATED TORUS KNOTS BOUNDING RATIONAL HOMOLOGY 4-BALLS
Errata

Lisa Lokteva
University of Glasgow
e.lokteva.1@research.gla.ac.uk

19th October 2023

- Page 2, line 12: In the paper, we have used [Don83, Theorem 1] as a reference for Donaldson's diagonalisation theorem. However, [Don83, Theorem 1] has the additional assumption that X be simply connected, which is done away with in [Don87, Theorem 1].
- Page 3, line -2: "The reason only one of the two families of cables with positive surgeries bounding torus knots mentioned in [AGLL20, Theorem 1.3] appears is that the other family has surgery coefficient lower than $p_2\alpha_2$." should say "Since $S^3_{(p_1+1)^2}T(p_1, p_1+1)$ and $S^3_{16}T(2,7)$ bound rational homology balls, [AGLL20, Theorem 1.3] predicts that $S^3_{p_2^2(p_1+1)^2}T(p_1, p_1+1; p_2, p_2(p_1+1)^2 \pm 1)$ and $S^3_{16p_2^2}T(2,7; p_2, 16p_2^2 \pm 1)$ will do so too. The reason half of these do not appear in the statement of Theorem 2 is that their surgery coefficient is lower than $p_2\alpha_2$."
- Page 6, line -3: "describes" should be "describe".
- Page 7, line -15: The end of proof symbol should not be there.
- Page 7, line -7: "Leaf node" should be "leaf vertex".
- Page 9, line 8: The "Proof" environment should not start. This is the continuation of the proof on page 7.
- Page 10, proposition 7: "positive iterated torus knot" should be "algebraic knot".
- Page 12, line -1: "node" should be "trivalent vertex".
- Page 13, line -12: "less that" should be "less than".

References

[AGLL20] Paolo Aceto, Marco Golla, Kyle Larson, and Ana G. Lecuona. Surgeries on torus knots, rational balls, and cabling. *arXiv e-prints*, page arXiv:2008.06760, August 2020.

[Don83] S. K. Donaldson. An application of gauge theory to four dimensional topology. *J. Differential Geom.*, 18(2):279–315, 1983.

[Don87] S. K. Donaldson. The orientation of Yang-Mills moduli spaces and 4-manifold topology. *Journal of Differential Geometry*, 26(3):397 – 428, 1987.

Paper I has been removed due to Copyright restrictions.

Paper II

Constructing Rational Homology 3-Spheres That Bound Rational Homology 4-Balls

University of Glasgow

Lisa Lokteva

19th October 2023

Abstract

We present two large families of new examples of plumbed 3-manifolds that bound rational homology 4-balls. These are constructed using two operations, also defined here, that preserve an algebraic obstruction to bounding rational homology balls. Apart from in the cases shown in this paper, it remains open whether these operations are rational homology cobordisms in general.

The families of new examples include a multitude of families of rational surgeries on torus knots, and we explicitly describe which positive torus knots we now know to have a surgery that bounds a rational homology ball.

While not the focus of this paper, we implicitly confirm the slice-ribbon conjecture for new, more complicated, examples of arborescent knots, including many Montesinos knots.

1 Introduction

In Kirby's problem 4.5 [13], Casson asks which rational homology 3-spheres bound rational homology 4-balls. While rational homology 3-spheres abound in nature, including the r-surgery $S^3_r(K)$ on a knot K for any $r \in \mathbb{Q} - \{0\}$, very few of them actually bound rational homology balls. In fact, Aceto and Golla showed in [2, Theorem 1.1], that for every knot K and every $q \in \mathbb{Z}_+$, there exist at most finitely many $p \in \mathbb{Z}_+$ such that $S^3_{p/q}(K)$ bounds a rational homology ball. It is hard to answer Casson's question in full generality, but recently a great deal of progress has been made on specific classes of rational homology 3-spheres. For example, in 2007 we learnt the answer for lens spaces [16, 17], in 2020 for positive integral surgeries on positive torus knots [2, 3], and in between we learnt the answer for several other classes on Seifert fibred spaces with three exceptional fibres [14, 15]. We do not yet know the answer for general Seifert fibred spaces with three exceptional fibres. In [18], the author started studying surgeries on algebraic (iterated torus) knots, which are not Seifert fibred but decompose into Seifert fibred spaces when cut along a maximal system of incompressible tori [12].

An important tool to study which 3-manifolds bound rational homology balls is the following corollary of Donaldson's diagonalisation theorem [8, Theorem 1]:

Theorem 1 (Corollary of Donaldson's Theorem)**.** *Let Y be a rational homology 3-sphere and $Y = \partial X$ for X a negative definite smooth connected oriented 4-manifold. If $Y = \partial W$ for a smooth rational homology 4-ball W, then there exists a lattice embedding*

$$(H_2(X)/\operatorname{Torsion}, Q_X) \hookrightarrow (\mathbb{Z}^{\operatorname{rk} H_2(X)}, -\operatorname{Id}).$$

Here Q_X is the intersection form on $H_2(X)/\operatorname{Torsion}$. Determining which 3-manifolds in a family $\mathfrak{F}$ bound rational homology 4-balls using lattice embeddings often goes like this:

(i) Find a negative-definite filling $X(Y)$ for every $Y \in \mathfrak{F}$.

(ii) Guess the family $\mathfrak{F}' \subset \mathfrak{F}$ of manifolds whose filling's intersection lattice (that is second homology with the intersection form) embeds into the standard lattice of the same rank.

(iii) Show that $(H_2(X(Y)), Q_{X(Y)})$ does not embed into $(\mathbb{Z}^{b_2(X(Y))}, -\operatorname{Id})$ for any $Y \in \mathfrak{F} - \mathfrak{F}'$.

(iv) Hopefully prove that Y bounds a rational homology ball for any $Y \in \mathfrak{F}'$.

This process is sensitive at every step. There exist 3-manifolds without any definite fillings [10]. However, lens spaces, surgeries on torus knots and large surgeries on algebraic knots do have definite fillings. In fact, they all bound definite plumbings of disc bundles on spheres. Step (iv) is definitely not guaranteed to work either. For example, $S^3_{-m^2}(K)$ bounds the knot trace $D^4_{-m^2}(K)$ (D^4 with a $-m^2$-framed 2-handle glued along K) which has intersection lattice $(\mathbb{Z}, (-m^2))$ which embeds into $(\mathbb{Z}, -\operatorname{Id})$, but according to [2, Theorem 1.2], $S^3_{-m^2}(K)$ bounds a rational homology ball for at most two positive integer values of m. However, in [16, 17, 2, 3] the authors managed to find an $X(Y)$ for each Y in such a way that the lattice embedding obstruction turned out perfect. These $X(Y)$s have been plumbings of disc bundles on spheres with a tree-shaped plumbing graph, moreover satisfying the property that the quantity

$$I = \sum_{v \in V} (-w(v) - 3),$$

where V is the set of vertices of the graph and $w(v)$ is the weight of v, would be negative.

Steps (ii) and (iii) can sometimes be done at the same time, but often, like in [3] where $\mathfrak{F}$ is the set of positive integral surgeries on positive torus knots, they cannot. It is then important to eliminate embeddable cases early in order to proceed with step (iii). Theorem 1.1 in [3], the classification of positive integral surgeries on positive torus knots bounding rational homology balls, lists 5 families that are Seifert fibred spaces with 3 exceptional fibres. They bound a negative-definite star-shaped plumbing with three legs. Families (1)-(3) have two complementary legs,

that is two legs whose weight sequences are Riemenschneider dual (defined, for the reader's convenience, in Section 2 of this paper). All such 3-manifolds that bound a rational homology ball have been classified by Lecuona in [14]. Family (5) contains two exceptional graphs which were known to bound rational homology balls both because they arise as boundaries of tubular neighbourhoods of rational cuspidal curves in [9] and because they are surgeries on torus knots $T(p,q)$ where $q \equiv \pm 1 \pmod{p}$, which were studied in [2]. However, Family (4) took the authors of [3] a while to find, in the meantime thwarting their attempts at step (iii). Eventually they found Family (4) using a computer. This allowed them to finish off their lattice embedding analysis, but Family (4) still looked surprising and strange and begged the question of "How could we have predicted its existence?"

1.1 GOCL and IGOCL Moves

This work came out of widening the perspective and asking which boundaries of 4-manifolds described by plumbing trees with negative definite intersection forms and low I bound rational homology balls. In particular, we asked ourselves which plumbing trees generate an embeddable intersection lattice. We looked at what the graphs of 3-manifolds we know to bound rational homology balls look like and tried to see if there are any common patterns. In [15, Remark 3.2], Lecuona describes how to get all lens spaces that bound rational homology balls from the linear graphs $(-2,-2,-2)$, $(-3,-2,-3,-3,-3)$, $(-3,-2,-2,-3)$ and $(-2,-2,-3,-4)$ using some modifications. (She restates Lisca's result in [16] in the language of plumbing graphs rather than fractions p/q for $L(p,q)$.) In this paper we define a couple of moves called GOCL and IGOCL moves on embedded plumbing graphs that preserve embeddability and generalise the moves described by Lecuona. From this point of view, Lecuona's list simply turns into a list of IGOCL and GOCL moves that keep the graph linear. The IGOCL move was also used by Jonathan Simone in [23] under the name of expansions. The GOCL move is a generalisation of Lisca's expansions in [16].

We may then ask ourselves if these moves preserve the property of the described 3-manifolds bounding rational homology balls. There is unfortunately no obvious rational homology cobordism between two 3-manifolds differing by a GOCL or an IGOCL move. We can however prove that repeated applications of these moves to the embeddable linear graphs $(-3,-2,-3,-3,-3)$ and $(-3,-2,-2,-3)$ give 3-manifolds bounding rational homology balls. We get the following theorem:

Theorem 2. *All 3-manifolds described by the plumbing graphs in Figures 1 and 2 bound rational homology balls.*

Remark. See Definition 12 for the definition of *complementary*.

In fact, we prove this theorem by showing that the above plumbed 3-manifolds bound a double cover of D^4 branched over a χ-slice link [7, Definition 1]. By [7, Proposition 5.1], this must be a rational homology 4-ball. At the same time, we show that these links are χ-ribbon.

Our method of showing that our 3-manifolds are double branched covers over χ-slice links appears to fail for the 3-manifolds described by plumbing graphs ob-

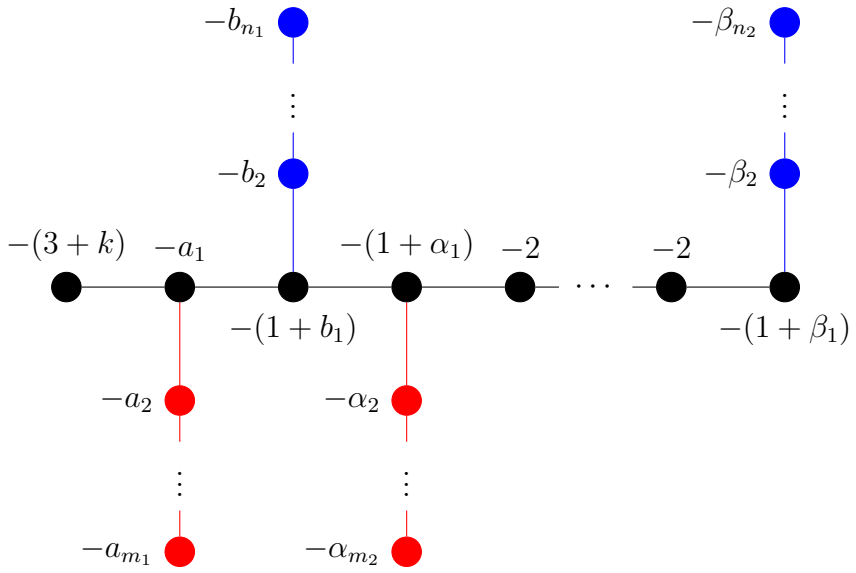

Figure 1: These are the graphs obtainable by performing IGOCL and GOCL moves on the linear graph $(-3,-2,-3,-3,-3)$. Here the length of the chain of -2's is $k \geq 0$, $(a_1,\ldots,a_{m_1})$ and $(\alpha_1,\ldots,\alpha_{m_2})$ are complementary sequences, and $(b_1,\ldots,b_{n_1})$ and $(\beta_1,\ldots,\beta_{n_2})$ are complementary sequences.

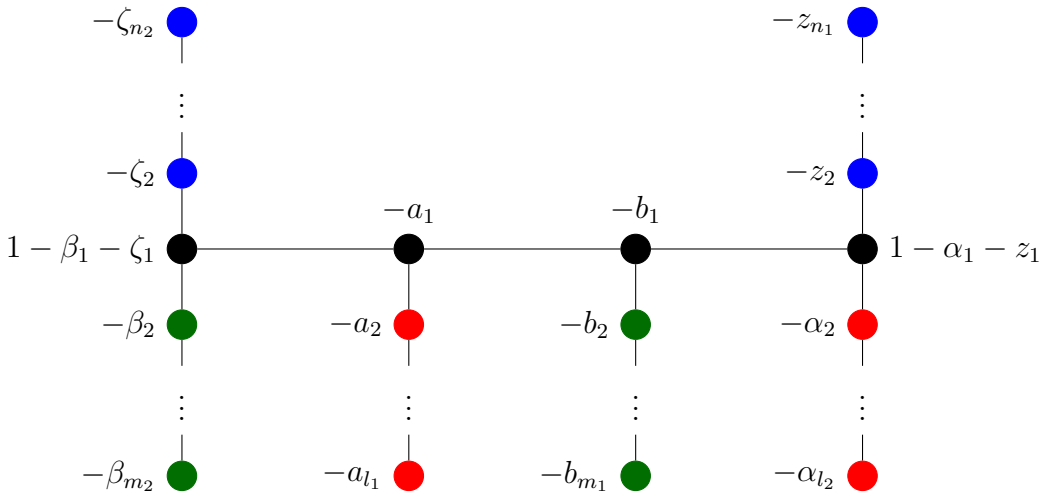

Figure 2: The form of all graphs obtainable from $(-3,-2,-2,-3)$ using GOCL moves. Here the sequences $(a_1,\ldots,a_{l_1})$ and $(\alpha_1,\ldots,\alpha_{l_2})$ are complementary, as well as the sequences $(b_1,\ldots,b_{m_1})$ and $(\beta_1,\ldots,\beta_{m_2})$, and the sequences $(z_1,\ldots,z_{n_1})$ and $(\zeta_1,\ldots,\zeta_{n_2})$.

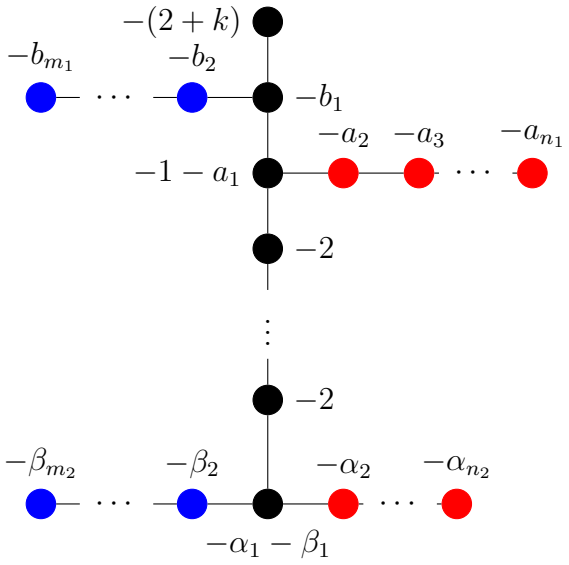

Figure 3: General expansion of Lisca's $(-2,-2,-3,-4)$ graph by GOCL and IGOCL moves. Here $1/[a_1,\dots,a_{n_1}]^- + 1/[\alpha_1,\dots,\alpha_{n_2}]^- = 2$; in other words $[a_1,\dots,a_{n_1}]^-$ and $[\alpha_1,\dots,\alpha_{n_2}]^-$ are complementary. The fractions $[b_1,\dots,b_{m_1}]^-$ and $[\beta_1,\dots,\beta_{m_2}]^-$ are complementary as well. The length of the chain of -2's is k.

tainable by GOCL and IGOCL moves from the $(-2,-2,-3,-4)$ linear graph. Nevertheless, we believe the following to be true:

Conjecture 3. *All 3-manifolds described by the plumbing graph in Figure 3 bound rational homology balls.*

The families of Figures 1, 2 and 3, together with the one generated from $(-2,-2,-2)$ which only contains linear graphs already found by Lisca, include all lens spaces bounding rational homology balls. They also contain more complicated graphs. In [1], Aceto defines linear complexity of a plumbing tree to be the minimal number of vertices we need to remove in order to get a linear graph. The families of Figures 3, 2 and 1 have linear complexities up to 2. Many papers, e.g. [1, 2, 3, 15, 23], using lattice embeddings to obstruct plumbed 3-manifolds from bounding a rational homology ball have used arguments of the form "If my graph Γ is embeddable, then this other linear graph obtained from Γ is embeddable, and we know what those look like.", which gets harder to do the further Γ is away from being linear. Thus we only really have lattice embedding obstructions so far for families of graphs of complexity 1. The families of Theorem 2 include many graphs of Seifert fibred spaces. They include Family (4) in [3] and predict its existence because Family (4) is just the intersection between the set of graphs in Figures 3, 2 and 1 and the negative-definite plumbing graphs of positive integral surgeries on positive torus knots.

As mentioned above, there is no obvious rational homology cobordism between the 3-manifolds described by two plumbing graphs differing by a GOCL or an IGOCL move. This is interesting in comparison with the case in the works by Aceto [1] and Lecuona [14]. Lecuona shows that given a plumbing graph Γ, you can

modify it to a graph Γ' by subtracting 1 from the weight of a vertex v and attaching two complementary legs $(-a_1, \ldots, -a_m)$ and $(-b_1, \ldots, -b_n)$ (see Section 2 or [14] for definitions) to v, and the 3-manifolds Y_Γ and $Y_{\Gamma'}$ described by the graphs will be rational homology cobordant, that is bound a rational homology 4-ball if and only if the other one does. Thus, if she wants to know if a $Y_{\Gamma'}$, for Γ' a graph with two complementary legs coming out of the same vertex, bounds a rational homology ball, she can reduce it to the same question for a simpler graph. However, since we do not know if the $GOCL$ and $IGOCL$ moves are rational homology cobordisms, we cannot play this trick for complementary legs growing out of different vertices.

Another work that has shown that applying GOCL moves to embedded plumbing graphs bounding certain rational homology balls gives us new plumbed 3-manifolds that bound rational homology balls is [4]. They show that the families $\Sigma(2, 4n+1, 12n+5)$ and $\Sigma(3, 3n+1, 12n+5)$ of Brieskorn spheres bound rational homology balls. In fact, these families are obtained by applying GOCL moves to the plumbing graphs of $\Sigma(2, 5, 17)$ and $\Sigma(3, 4, 17)$. Just like us in Section 3, they perform a -1-surgery on their spaces and the result of this surgery is the same for each space. Unlike us, they use this to show that the families $\Sigma(2, 4n+1, 12n+5)$ and $\Sigma(3, 3n+1, 12n+5)$ are surgeries on the 0-surgery on a rationally slice knot, which by [4, Lemma 2] implies that they bound rational homology balls. Reconciling our approaches is an interesting direction for future research.

1.2 Rational Surgeries on Torus Knots

An interesting generalisation of [3, Theorem 1.1], would be to classify all positive rational surgeries on positive torus knots that bound rational homology balls. Theorem 2 allows us to construct more examples of such surgeries than is sightly to write down. Instead, we may ask ourselves the following question:

Question 4. *For which $1 < p < q$ with $\mathrm{GCD}(p, q) = 1$ is there an $r \in \mathbb{Q}_+$ such that $S^3_r(T(p, q))$ bounds a rational homology ball?*

Section 4 is dedicated to showing the following theorem:

Theorem 5. *For the following pairs (p, q) with $1 < p < q$ and $\mathrm{GCD}(p, q) = 1$, there is at least one $r \in \mathbb{Q}_+$ such that $S^3_r(T(p, q))$ bounds a rational ball. Here $k, l \geq 0$.*

1. $(k+2, (l+1)(k+2)+1)$
2. $(k+2, (l+2)(k+2)-1)$
3. $(2k+3, (l+1)(2k+3)+2)$
4. $(2k+3, (l+2)(2k+3)-2)$
5. $(k^2+7k+11, k^3+12k^2+45k+51)$
6. $(S^{(k)}_{l+1}, S^{(k)}_{l+2})$ *for* $(S^{(k)}_i)$ *a sequence defined by* $S^{(k)}_0 = 1$, $S^{(k)}_1 = 2$, $S^{(k)}_2 = 2k+7$ *and* $S^{(k)}_{i+2} = (k+4)S^{(k)}_{i+1} - S^{(k)}_i$.

7. $(T^{(k)}_{l+1}, T^{(k)}_{l+2})$ *for* $(T^{(k)}_i)$ *a sequence defined by* $T^{(k)}_0 = 1$, $T^{(k)}_1 = k+2$, $T^{(k)}_2 = k^2+6k+7$ *and* $T^{(k)}_{i+2} = (k+4)T^{(k)}_{i+1} - T^{(k)}_i$.

8. (U_{l+1}, U_{l+2}) *for* (U_i) *a sequence defined by* $U_0 = 1$, $U_1 = 3$, $U_2 = 14$ *and* $U_{i+2} = 5U_{i+1} - U_i$.

9. (R_{l+1}, R_{l+2}) *for* (R_i) *a sequence defined by* $R_0 = 1$, $R_1 = 3$, $R_2 = 17$ *and* $R_{i+2} = 6R_{i+1} - R_i$.

10. $(A, (n+1)Q+P)$ *for* P *and* Q *such that* $L(Q,P)$ *bounds a rational homology ball (or equivalently* $\frac{Q}{P}$ *lying in Lisca's set* $\mathcal{R}$ *[16]), and* A *a multiplicative inverse to either* Q *or* $nQ+P$ *modulo* $(n+1)Q+P$ *such that* $0 < A < (n+1)Q+P$.

11. $((n+1)Q+P, (l+1)((n+1)Q+P)+A)$ *for* P *and* Q *such that* $L(Q,P)$ *bounds a rational homology ball (or equivalently* $\frac{Q}{P}$ *lying in Lisca's set* $\mathcal{R}$ *[16]), and* A *a multiplicative inverse to either* Q *or* $nQ+P$ *modulo* $(n+1)Q+P$ *such that* $0 < A < (n+1)Q+P$.

12. (B, P) *for* P *and* Q *such that* $L(Q,P)$ *bounds a rational homology ball (or equivalently* $\frac{Q}{P}$ *lying in Lisca's set* $\mathcal{R}$ *[16]), and* B *a multiplicative inverse to either* $P\lceil\frac{Q}{P}\rceil - Q$ *or* $Q - P\lfloor\frac{Q}{P}\rfloor$ *modulo* P *such that* $0 < B < P$.

13. $(P, (l+1)P+B)$ *for* P *and* Q *such that* $L(Q,P)$ *bounds a rational homology ball (or equivalently* $\frac{Q}{P}$ *lying in Lisca's set* $\mathcal{R}$ *[16]), and* B *a multiplicative inverse to either* $P\lceil\frac{Q}{P}\rceil - Q$ *or* $Q - P\lfloor\frac{Q}{P}\rfloor$ *modulo* P *such that* $0 < B < P$.

14. (P, Q) *such that there is a number* n *such that* $(P, Q, n) \in \mathcal{R} \sqcup \mathcal{L}$ *for the sets* $\mathcal{R}$ *and* $\mathcal{L}$ *defined in [3, Theorem 1.1]. (Note that here* $r = n \in \{PQ, PQ-1, PQ+1\}$*, so we are looking at an integral surgery.)*

If Conjecture 3 is true, then the following would follow:

Theorem 6. *If Conjecture 3 is true, then for the following pairs* (p,q) *with* $1 < p < q$ *and* $\mathrm{GCD}(p,q) = 1$*, there is at least one* $r \in \mathbb{Q}_+$ *such that* $S^3_r(T(p,q))$ *bounds a rational ball. Here* $k, l \geq 0$.

1. (P_{l+1}, P_{l+2}) *for* (P_i) *a sequence defined by* $P_0 = 1$, $P_1 = 4$, $P_2 = 19$ *and* $P_{i+2} = 5P_{i+1} - P_i$.

2. (Q_{l+1}, Q_{l+2}) *for* (Q_i) *a sequence defined by* $Q_0 = 1$, $Q_1 = 2$, $Q_2 = 9$ *and* $Q_{i+2} = 5Q_{i+1} - Q_i$.

The interested reader can use the methods of Section 4 to obtain the surgery coefficients r too.

In Theorem 5, case 14 is shown to bound rational homology balls in [3] and reflects the degenerate cases of surgeries on torus knots that are lens spaces or connected sums of lens spaces, cases 10-13 are shown to bound rational homology balls in [14] because their graphs have a pair of complementary legs, while the cases 1-8 are shown to bound rational homology balls in this paper, using that there

exists an r such that $S^3_r(T(p,q))$ bounds a graph in the families of Figures 2 and 1. Case 9 is not obtainable from Theorem 2 but Conjecture 3. However, we know that it bounds a rational homology ball from [3, Theorem 1.1 (4)]. The authors of [3] classified all positive integral surgeries on positive torus knots that bound rational homology balls. The classification included 18 families, whereof families (6)-(18) are included in our family 14, family (4) in our family 9, and the others in families 1 and 2.

At the moment of writing we do not know of any other positive torus knots having positive surgeries bounding rational homology balls. The pair $(8,19)$ is in some metric the smallest example not to appear on the list of Theorem 5. Thus we may concretely ask:

Question 7. *Is there an $r \in \mathbb{Q}_+$ such that $S^3_r(T(8,19))$ bounds a rational homology ball?*

We may also note that some positive torus knots have many surgeries that bound rational homology balls. For example, Theorem 2 allows us to construct numerous finite and infinite families of surgery coefficients $r \in \mathbb{Q}_+$ such that $S^3_r(T(2,3))$ bounds a rational homology ball. All we need to do is to choose weights in the graphs in Figures 1 and 2 so that we get a starshaped graph with three legs whereof one is (-2) and another is either $(-2,-2)$ or (-3). For example, $S^3_{\frac{(6k+5)^2}{6k^2+9k+3}}(T(2,3))$ bounds a plumbing of the shape in Figure 2 with $(a_1,\dots,a_{l_1}) = (2+k,2)$, $(b_1,\dots,b_{m_1}) = (2)$ and $(z_1,\dots,z_{n_1}) = (2)$, $k \geq 1$, and thus bounds a rational homology ball for any $k \geq 1$. There are also surgeries on $T(2,3)$ that bound rational balls, but do not have graphs of the shapes of Figures 1, 2 or 3. For example, $S^3_{\frac{64}{7}}(T(2,3)) = -S^3_{64}(T(3,22))$, which bounds a rational homology ball because it is the boundary of the tubular neighbourhood of a rational curve in $\mathbb{C}P^2$ [9], but whose lattice embedding contains a basis vector with coefficient 2, which we do not get by applying $GOCL$ or $IGOCL$ moves to $(-2,-2,-3,-4)$, $(-3,-2,-2,-3)$ and $(-3,-2,-3,-3,-3)$. The lattice embedded plumbing graph of $S^3_{\frac{64}{7}}(T(2,3))$ does however fit into Family $\mathcal{C}$ of [24] of symplectically embeddable plumbings. Unfortunately, Family $\mathcal{C}$ of [24] contains both surgeries on $T(2,3)$ that bound rational homology balls and ones that do not. For example, $S^3_{\frac{169}{25}}(T(2,3))$ of [24, Section 2.4, Figure 12] does not bound a rational ball despite bounding a plumbing with an embeddable intersection form. A later paper [6] classified which surgeries on $T(2,3)$ appearing in Family $\mathcal{C}$, viewed as surface singularity links, bound a rationally acyclic Milnor fibre. Interestingly, all but two of the embedded graphs in that family are generated by applying IGOCL moves to the graph of $S^3_{\frac{64}{7}}(T(2,3))$. However, we do not know if any other members of Family $\mathcal{C}$ bound a rational homology ball which is not a Milnor fibre. Hence, the following is a rich open question worth studying:

Question 8. *For which $r \in \mathbb{Q}_+$ does $S^3_r(T(2,3))$ bound a rational homology ball?*

1.3 Outline

We start off the paper with Section 2 by recalling some results on complementary legs and the basics of the lattice embedding setup. In Section 3 we define the GOCL

and IGOCL moves and show Theorem 2. In Section 4 we prove Theorem 5 for the families 1-11, while the other families follow directly from [14] and [3].

2 Complementary Legs and Lattice Embeddings

In this section we list some definitions and easy propositions that are helpful to understanding the paper. We recall the definition of lattice embeddings and apply it to chain graphs and complementary legs.

Definition 9. *A chain graph is a simple graph with $\mathbb{Z}$-weighted vertices and $\{+1,-1\}$-weighted edges, together with a particular embedding into $\mathbb{R}^2$.*

Given a chain graph Γ with weight function $W : V \to \mathbb{Z}$, we associate to it a 4-manifold X_Γ by describing its Kirby diagram. First, we draw a small unknot, oriented anti-clockwise, at each vertex of Γ. Then, for each edge, we create a Hopf linking between the knots corresponding to the edge ends as in Figure 4. We denote the resulting link by L_Γ. Then X_Γ is the simply-connected 4-manifold obtained by attaching 2-handles with framing $W(v)$ to the unknot at each vertex v.

We denote the 3-manifold ∂X_Γ by Y_Γ.

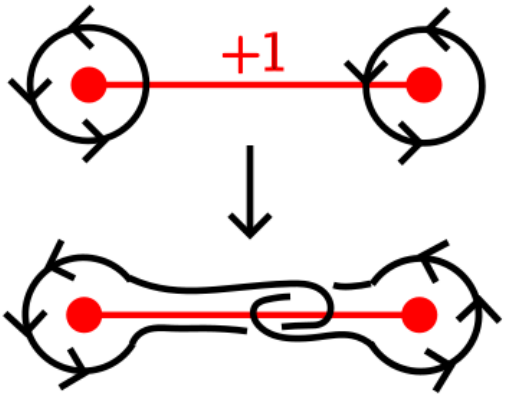

Figure 4: Construction of the 4-manifold X_Γ associated to a chain graph Γ. For each $+1$-edge, we create a positive Hopf linking between the corresponding unknots as in this figure. For each -1-edge, we create a negative Hopf linking instead.

Remark 9.1. Note that if Γ is a tree, then the definition of a chain graph coincides with the definition of a plumbing graph (see [11, Example 4.6.2]).

Remark 9.2. It is useful to study which pairs of graphs (Γ, Γ') give $X_\Gamma \cong X_{\Gamma'}$ and $Y_\Gamma \cong Y_{\Gamma'}$. Obviously, $X_\Gamma \cong X_{\Gamma'}$ if Γ is isotopic to Γ'. However, we need to take care when changing the order of the edges around a vertex. This can sometimes be done, which can be seen by translating into Kirby calculus.

Remark 9.3. A common abuse of terminology is "the chain graph Γ bounds a rational homology ball", which means that Y_Γ bounds a rational homology ball.

Let Γ be a chain graph. The second homology of X_Γ is the free abelian group $\mathbb{Z}\langle V_1, \dots, V_k\rangle$ on the vertices and the intersection form is

$$\langle V_i, V_j\rangle_{Q_X} = \begin{cases} \text{weight of } V_i & \text{if } i = j \\ \operatorname{sign} e_{ij} & \text{if } V_i \text{ is adjacent to } V_j \text{ through edge } e_{ij} \\ 0 & \text{otherwise.} \end{cases}$$

Definition 10. *Let X be a 4-manifold with boundary. A* lattice embedding

$$f : (H_2(X)/\operatorname{Torsion}, Q_X) \hookrightarrow (\mathbb{Z}^N, -\operatorname{Id})$$

is a linear map f such that $\langle V_i, V_j\rangle_{Q_X} = \langle f(V_i), f(V_j)\rangle_{-\operatorname{Id}}$. We will simply denote $\langle\cdot,\cdot\rangle := \langle\cdot,\cdot\rangle_{-\operatorname{Id}}$. If nothing else is specified, then $N = \operatorname{rk} H_2(X)$, that is the number of vertices in the graph.

Common abuses of notation include "embedding of the graph", meaning an embedding of the lattice $(H_2(X)/\operatorname{Torsion}, Q_X)$, where X is described a chain graph.

Knowing when a lattice embedding exists is useful because of Theorem 1 in the introduction.

Now we turn our heads to lattice embeddings of specific chain graphs, namely pairs of complementary legs.

Definition 11. *We define the negative continued fraction $[a_1, \dots, a_n]^-$ as*

$$[a_1, \dots, a_n]^- = a_1 - \cfrac{1}{a_2 - \cfrac{1}{\ddots - \cfrac{1}{a_n.}}}$$

Negative continued fractions often show up in low-dimensional topology because of the slam-dunk Kirby move [11, Figure 5.30], which allows us to substitute a rational surgery on a knot by an integral surgery on a link.

Definition 12. *A two-component weighted linear graph $(-\alpha_1, ..., -\alpha_n), (-\beta_1, ..., -\beta_k)$ (with α_i, β_j integers greater than or equal to 2) is called a pair of complementary legs if*

$$\frac{1}{[\alpha_1, ..., \alpha_n]^-} + \frac{1}{[\beta_1, ..., \beta_k]^-} = 1.$$

We call the sequence $(\beta_1, ..., \beta_k)$ the Riemenschneider dual or complement of the sequence $(\alpha_1, ..., \alpha_n)$, and we call the fractions $[\alpha_1, ..., \alpha_n]^-$ and $[\beta_1, ..., \beta_k]^-$ complementary.

Definition 13. *A Riemenschneider diagram is a finite set of points S in $\mathbb{Z}_+ \times \mathbb{Z}_-$ such that $(1, -1) \in S$ and for every point $(a, b) \in S$ but one, exactly one of $(a+1, b)$ or $(a, b-1)$ is in S. If $(n, k) \in S$ is the point with the largest $n - k$, we say that the Riemenschneider diagram represents the fractions $[\alpha_1, ..., \alpha_n]^-$ and $[\beta_1, ..., \beta_k]^-$, where α_i is one more than the number of points with $x = i$ and β_j is one more than the number of points with $y = -j$.*

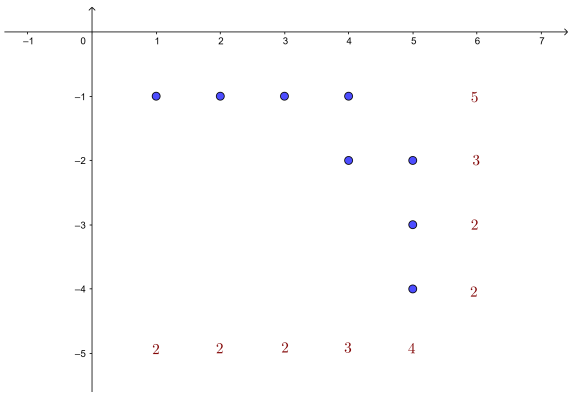

Figure 5: Example of a Riemenschneider diagram representing the complementary fractions $[5,3,2,2]^-$ and $[2,2,2,3,4]^-$.

Example 14. See Figure 5 for an example of a Riemenschneider diagram.

Proposition 15 (Riemenschneider [22])**.** *The two fractions represented by a Riemenschneider diagram are complementary.*

Remark 15.1. Note that given any continued fraction $[\alpha_1, ..., \alpha_n]^-$ with all $\alpha_i \geq 2$, we may construct a Riemenschneider diagram representing $[\alpha_1, ..., \alpha_n]^-$ and its Riemenschneider dual.

The following theorem is well-known, but we explicitly write out the embedding construction for the reader's convienience.

Proposition 16. *Every pair of complementary legs has a lattice embedding.*

Proof. The embedding can be constructed algorithmically from a Riemenschneider diagram. Denote the vertices of the two complementary legs by $(U_1, \ldots, U_{m_1})$ and $(V_1, \ldots, V_{m_2})$. These vertices generate the second homology of the plumbed 4-manifold described by the graph. We need to send every vertex to an element of $\mathbb{Z}\langle e_1, \ldots, e_{m_1+m_2}\rangle$. Start by mapping both U_1 and V_1 to e_1. Order the points in the Riemenschneider diagram so that $P_1 = (1, -1)$, and if $P_i = (a, b)$, then point P_{i+1} is either $(a+1, b)$ or $(a, b-1)$. Now, we recursively build an embedding as follows. For each non-final i, if the current partial embedding is $(u_1, ..., u_n), (v_1, ..., v_k)$ (meaning that $(U_1, \ldots, U_n)$ gets mapped to $(u_1, ..., u_n)$ and $(V_1, \ldots, V_k)$ gets mapped to $(v_1, \ldots, v_k)$) and $P_i = (a, b)$ is such that $P_{i+1} = (a + 1, b)$, then the new partial embedding will be $(u_1, ..., u_n + e_{i+1}), (v_1, ..., v_k - e_{i+1}, e_{i+1})$. If $P_{i+1} = (a, b-1)$, then the new partial embedding will be $(u_1, ..., u_n - e_{i+1}, e_{i+1}), (v_1, ..., v_k + e_{i+1})$ instead. If P_i is final and the current partial embedding is $(u_1, ..., u_n), (v_1, ..., v_k)$, the new embedding will be $(u_1, ..., u_n + e_{i+1}), (v_1, ..., v_k - e_{i+1})$, or the other way around, whatever is preferred. It is easy to see that an embedding $(u_1, ..., u_{m_1}), (v_1, ..., v_{m_2})$ constructed this way will have the properties:

- Each u_i for $i = 1, ..., n-1$ and v_j for $j = 1, ..., k$ will be a sum of consecutive basis vectors, all but the last one with coefficient 1, and the last one with coefficient -1. Meanwhile u_n will be a sum of consecutive basis vectors all with coefficient 1.

- If the Riemenschneider diagram represents the fractions $[\alpha_1, ..., \alpha_n]^-$ and $[\beta_1, ..., \beta_k]^-$, then $\langle u_i, u_i \rangle = -\alpha_i$ and $\langle v_j, v_j \rangle = -\beta_j$.
- Since u_i and u_{i+1} have exactly one basis vector in common, one with a positive coefficient and one with a negative one, $\langle u_i, u_{i+1} \rangle = 1$, and similarly $\langle v_i, v_{i+1} \rangle = 1$.
- The other pairs (u_i, u_j) (with $|i - j| > 1$) don't share basis vectors and are thus orthogonal. Similarly, the pairs (v_i, v_j) with $|i - j| > 1$ don't share basis vectors and are thus orthogonal.
- It is easy to show by induction on the construction that $\langle u_i, v_j \rangle = 0$ for all i, j.

These properties show that we are in fact looking at a lattice embedding of the complementary legs. □

Remark 16.1. In fact, if e_1 is fixed to hit the first vertex of each complementary leg, the rest of the embedding is unique up to renaming of elements and sign of the coefficient [5, Lemma 5.2].

The following facts are useful when dealing with lattice embeddings. We will often use these properties without citing them. The first fact follows from reversing the Riemenschneider diagram, the second from embedding the sequences $(a_m, \ldots, a_1)$ and $(b_n, \ldots, b_1)$ as in Theorem 16 and mapping the -1-weighted vertex to $-e_1$, and the rest from looking at a Riemenscheider diagram.

Proposition 17. *Let $(a_1, \ldots, a_m)$ and $(b_1, \ldots, b_n)$ be complementary sequences. Then the following hold:*

1. *The sequences $(a_m, \ldots, a_1)$ and $(b_n, \ldots, b_1)$ are complementary.*
2. *The linear graph $(-a_1, \ldots, -a_m, -1, -b_n, \ldots, -b_1)$ embeds in $(\mathbb{Z}^{m+n}, -\mathrm{Id})$.*
3. *Either a_m or b_n must equal 2, so assume without loss of generality that $b_n = 2$. Blowing down the -1 in the linear graph $(-a_1, \ldots, -a_m, -1, -b_n, \ldots, -b_1)$ gives us the linear graph $(-a_1, \ldots, -(a_m - 1), -1, -b_{n-1}, \ldots, -b_1)$. This graph is once again a pair of complementary legs linked by a -1, described by the Riemenschneider diagram obtained by the removing the last point.*
4. *Repeatedly blowing down the -1 in linear graphs of the form*

   $$(-a_1, \ldots, -a_m, -1, -b_n, \ldots, -b_1)$$

   eventually takes us to $(-2, -1, -2)$, or even further to $(-1, -1)$ or (0).
5. *Similarly, blowing up next to the -1 gives $(-a_1, \ldots, -(a_m+1), -1, -2, -b_n, \ldots, -b_1)$ or $(-a_1, \ldots, -a_m, -2, -1, -(b_n + 1), \ldots, -b_1)$, which are both pairs of complementary legs connected by a -1, described by Riemenschneider diagrams that are extensions of the initial one by one dot.*

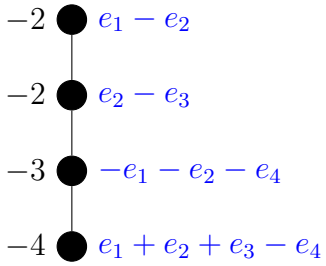

Figure 6: Lisca's $(-2,-2,-3,-4)$ graph with embedding.

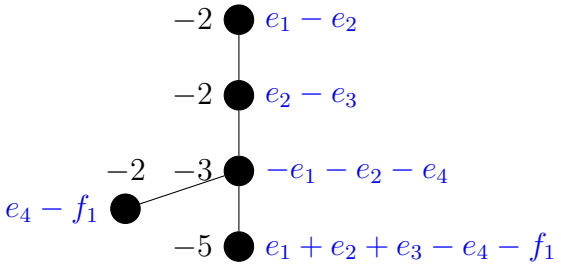

Figure 7: An extension of Lisca's $(-2,-2,-3,-4)$ graph with embedding.

3 Growing Complementary Legs on Lisca's Graphs

The idea for this work comes from studying the lattice embeddings of linear graphs and other trees that are known to bound rational homology 4-balls. Consider for example Lisca's classification of connected linear graphs that bound rational homology 4-balls [16], in the most convenient form for us described by Lecuona in [15, Remark 3.2]. Every family of embeddable graphs can be obtained from the basic graphs $(-2,-2,-2)$, $(-2,-2,-3,-4)$, $(-3,-2,-2,-3)$ and $(-3,-2,-3,-3,-3)$ by repeated application of two types of moves, one of which is the following: choose a basis vector e hitting exactly two vertices v and w, where w is **final** (Lisca's word for leaf, that is a vertex of degree 1 [16, p. 6]), subtract 1 from the weight of v and attach a new vertex u of weight -2 to w. In this section, we will show that if we start with any of the graphs $(-2,-2,-2)$, $(-3,-2,-2,-3)$ or $(-3,-2,-3,-3,-3)$, we can do away with the assumption that w is final and still get 3-manifolds bounding rational homology 4-balls through repeating this operation.

Example 18. Consider Figure 6, showing an embedding of Lisca's $(-2,-2,-3,-4)$ graph into the standard lattice $(\mathbb{Z}\langle e_1,e_2,e_3,e_4\rangle, -\mathrm{Id})$. Note that e_4 and e_3 hit two vertices each. Choose e_4. We can now perform the operation described above by choosing v to be the vertex of weight -4 and w the vertex of weight -3. The result is shown in Figure 7 together with its embedding, which is a kind of "expansion" of the embedding in Figure 6. Our new embedding has two basis vectors hitting exactly two vertices each, namely e_3 and f_1, whereas e_4 now hits three vertices. We may now perform the same operation again on any of these basis vectors, thereby obtaining any graph of the form described in Figure 3, with $k = 0$. We will show that these graphs do not only have lattice embeddings, but also bound rational homology 4-balls.

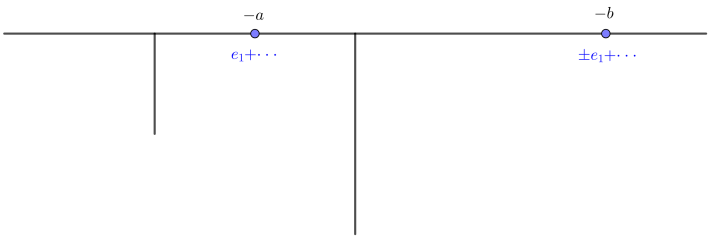

(a) Before GOCL.

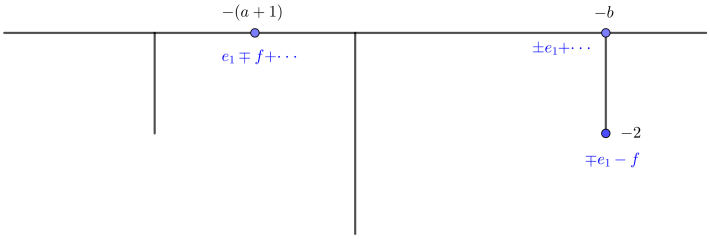

(b) After GOCL.

Figure 8: A GOCL move on a graph with a lattice embedding.

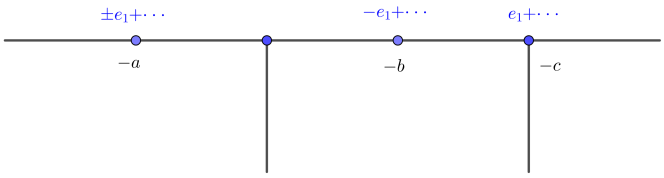

(a) Before IGOCL.

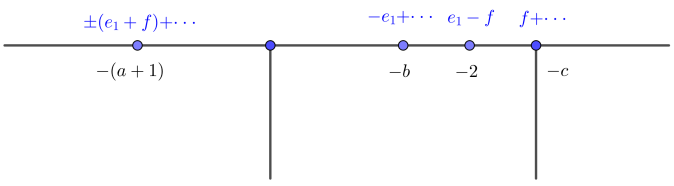

(b) After IGOCL.

Figure 9: An IGOCL move on a graph with a lattice embedding.

We will now introduce two moves on chain graphs with a lattice embedding. Let $\Gamma = (V, E, W)$ be a weighted negative-definite graph with lattice embedding $F : (V, Q_{X_\Gamma}) \to (\mathbb{Z}^{|V|}, -\mathrm{Id})$. Assume that there is a basis vector e of $\mathbb{Z}^{|V|}$ hitting exactly two vertices A and B in Γ, whose images are v and w, in any order we prefer. Then a **GOCL (growth of complementary legs) operation** is constructing an embedded graph $(\Gamma' = (V', E', W'), F')$ by $V' = V \cup C$, $E' = E \cup \{AC\}$ and $u := F'(C) = -\langle e, v\rangle e - f$, $w' := F'(B) = w - \langle e, v\rangle\langle e, w\rangle f$ and $F'(D) = F(D)$ for all $D \in V - \{B\}$. This move is illustrated by Figure 8. Note that $\langle e, v\rangle\langle e, w\rangle = \langle f, u\rangle\langle f, w'\rangle$. Thus, the GOCL operation substitutes e by f in the set of basis vectors hitting the graph exactly twice and moreover, the sign difference between the two occurrences of the basis vector is preserved. This operation can therefore be applied repeatedly. If we start with the graph consisting of two vertices of weight -2 and no edges, and the embedding $e_1 - e_2$ and $e_1 + e_2$, then repeated application of GOCL will simply give us two complementary legs.

The other operation which we will call **IGOCL (inner growth of complementary legs)** could be described as growing complementary legs from the inside. Suppose a basis vector e hits exactly three vertices A, B and C in Γ, with their images under the lattice embedding F being u, v and w respectively. Assume also that B and C are adjacent and that $\langle v, e\rangle\langle w, e\rangle = -1$, that is e hits v and w with opposite signs. Then $\Gamma' = (V', E', W')$ is described by $V' = V \cup \{D\}$, $E' = (E - \{BC\}) \cup \{BD, DC\}$, $F'(D) = -\langle v, e\rangle e + \langle v, e\rangle f$, $F'(C) = w - \langle w, e\rangle e + \langle w, e\rangle f$, $F'(A) = u + \langle u, e\rangle f$ and $F'(X) = F(X)$ for all $X \in V - \{A, C\}$. This operation is illustrated in Figure 9. After this operation is performed, we can perform it again on either e or f, but the result is essentially the same. What it does is grow a chain of -2's between two vertices and compensate by subtracting from the weight of a different vertex. If we apply the IGOCL operation on a vector hitting a pair of complementary legs three times, we still get a pair of complementary legs, which explains the name.

3.1 The Method to Show Theorem 2

Now that we have defined the GOCL and IGOCL moves, the remainder of this section will be dedicated to their applications to Lisca's basic graphs $(-2, -2, -2)$, $(-3, -2, -3, -3, -3)$ and $(-3, -2, -2, -3)$. We will show for these one by one that the results obtained from repeatedly applying the aforementioned operations always bound rational homology balls. This subsection details the method.

Recall Definition 9 and its notation. If Γ is a tree, then the link L_Γ is **strongly invertible** (defined in [19]), that is can always be drawn in a way equivariant with respect to the 180° rotation around the x-axis in such a way that every knot intersects the x-axis in exactly two points. (For example, see Figure 10.)

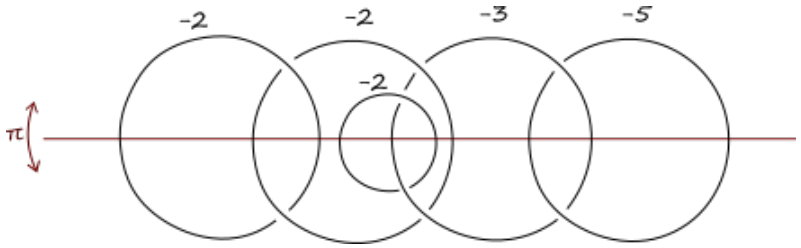

Figure 10: Proof that the attaching link of the graph in Figure 7 is strongly invertible.

Let $\pi : X_\Gamma \to X_\Gamma$ be the involution given by extending this 180° rotation around the x-axis and let $p : X_\Gamma \to X_\Gamma/\pi$ be the quotient map when we identify $x \sim \pi(x)$. By [19, Theorem 3], $X_\Gamma/\pi = B^4$ and p is a double covering, branched over a surface $S_\Gamma \subset B^4$. The surface S_Γ can be drawn by attaching bands to a disc according to the bottom half of the rotation-equivariant drawing, adding as many half-twists as the weight of the corresponding unknot [19]. (See Figure 11.) By K_Γ we denote the link $K_\Gamma = S_\Gamma \cap S^3$. Note that $K_\Gamma \neq L_\Gamma$.

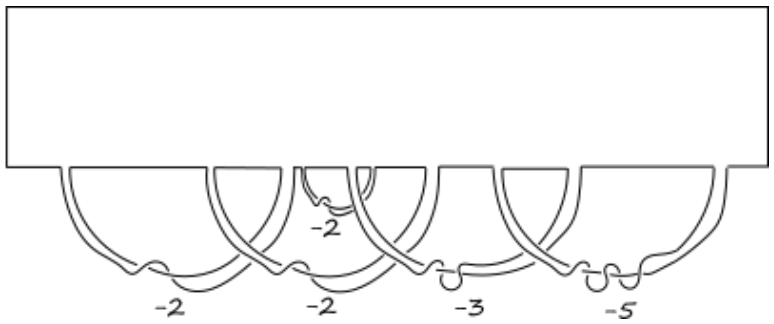

Figure 11: S_Γ for Γ the graph in Figure 7 is a disc with five bands attached.

We will show that if Γ is obtainable from the $(-3,-2,-3,-3,-3)$ or $(-3,-2,-2,-3)$ Lisca graphs by GOCL and IGOCL moves, then Y_Γ bounds a rational homology 4-ball. We will do this by showing that K_Γ is χ-slice, that is bounds a surface of Euler characteristic 1 inside B^4 [7, Definition 1]. The χ-sliceness will be proven by adding two (or one) 2-handles to X_Γ in a $\mathbb{Z}/2\mathbb{Z}$-equivariant fashion (changing the branching locus from S_Γ to a different surface S by adding two (or one) bands), in such a way that we obtain $(S^1 \times S^2)\#(S^1 \times S^2)$ (or $(S^1 \times S^2)$) and that ∂S is the 3-component (or 2-component) unlink. Addition of such bands is a concordance of boundary links. It will follow that K_Γ bounds an embedded surface $F = S \cup D^2 \cup D^2 (\cup D^2)$ in B^4 obtained from adding two (or one) bands to K_Γ and capping off with three (or two) discs, meaning that K_Γ is the boundary of a surface obtained from attaching two bands to three discs (or one band to two discs). This surface is homotopy equivalent to three points with two edges (or two points with one edge), which has Euler characteristic 1. We use [7, Proposition 5.1] to conclude that the double cover of B^4 branched over F is a rational homology ball with boundary Y_Γ.

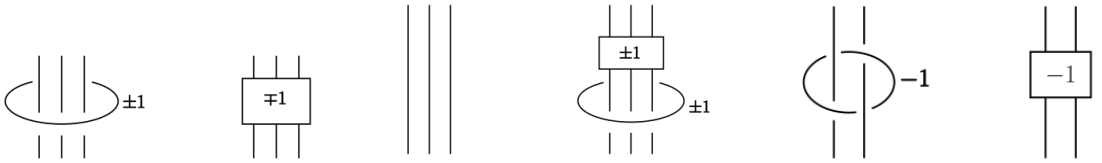

(a) Simple blow-down (b) Simple blow-up (c) Twisted blow-down

Figure 12: Useful blow-ups and blow-downs.

3.2 $(-2,-2,-2)$

This graph has embedding $(e_1-e_2, e_2-e_3, -e_1-e_2)$. The only basis vector hitting twice is e_1 whose both occurrences are in final vertices. Thus applying the GOCL operation keeps the graph linear and all such graphs have been shown to be bounding rational homology balls by Lisca. In fact, these graphs describe the lens spaces $L(p^2, pq\pm 1)$, for $p>q>0$ with some orientation [16, Lemma 9.2].

3.3 $(-3,-2,-3,-3,-3)$

In this subsection, we show the following proposition:

Proposition 19. *Every 3-manifold described by the graph in Figure 1 bounds a rational homology 4-ball.*

Let Γ be a graph as in Figure 1. By Subsection 3.1, we need to find a way to add a 2-handle to X_Γ in such a way that the boundary turns into $S^1\times S^2$, that is the 3-manifold described by the 0-surgery on an unknot. For this, we will work backwards and show that the 0-surgery on an unknot blows up to a surgery on Y_Γ.

The proof will be by Kirby calculus, so in Figure 12 we recall the effect of some blow-ups and blow-downs on Kirby diagrams. Recall that if there are k strands of a link component (counted with sign) in a bunch that we are about to perform a ± 1 blow up around, then the framing of that component increases by $\pm k^2$.

Now, we start by the chain

$$(-b_{n_1},\dots,-b_1,-(2+k),-1,\underbrace{-2,\dots,-2}_{k},-(1+\beta_1),-\beta_2,\dots,-\beta_{n_2}).$$

Note that it consists of two Riemenschneider dual chains connected by a -1, so by Proposition 17, it blows down to the (0) chain. Since the graph is a tree, the sign of the crossings doesn't matter yet. We will arrange the crossings around the $-(2+k)$-vertex as in Figure 13a. The chains $(-b_2,\dots,-b_{n_1})$ and $(-2,\dots,-2,-(1+\beta_1),-\beta_2,\dots,-b_{n_2})$, on the other hand, since they are not relevant to the Kirby moves that follow, are represented by tiny squares that freely move on their respective components.

Now we apply the Kirby calculus of Figure 13. The diagram in Figure 13c can no longer be described by a plumbing graph where every vertex is a link component. In fact, the red, blue, and black components form a triple Hopf link. Let us perform a blow-up at the clasp between the blue and the black components. This is a negative

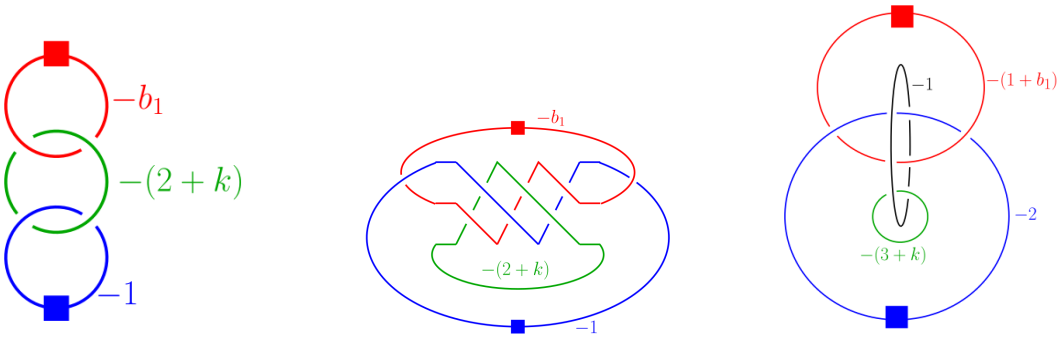

(a) Start (b) Isotope (c) Apply Figure 12a

Figure 13: Creating a 3-cycle.

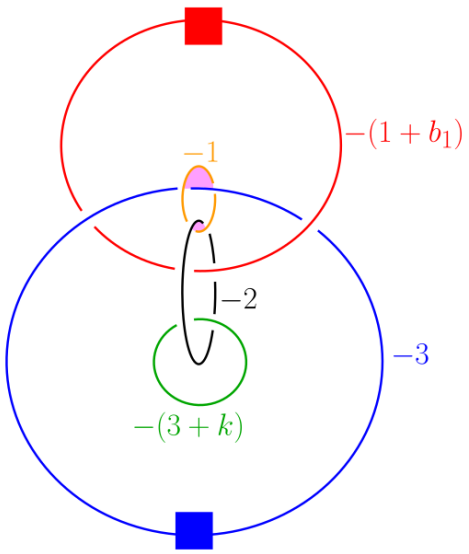

Figure 14

clasp, so we need to perform the twisted blow-up of Figure 12c. We obtain Figure 14.

Now note that removing the amber -1-knot in Figure 14 yields the Kirby diagram of Figure 1 with $(a_1, \dots, a_{m_1}) = (2)$. To obtain more general tuples $(a_1, \dots, a_{m_1})$, we will have to repeatedly blow up the clasps on the -1-weighted component. At the moment, both of these clasps in Figure 14 (in magenta) are negative and can be blown up using Figure 12c, an operation that substitutes a clasp by a -1-weighted ring with two negative clasps on either side. Thus, repeated blow-ups will give us a figure like Figure 14, but with the amber ring potentially substituted by a longer chain. In any case, the link in this figure is strongly invertible, and removing the -1-weighted component yields the Kirby diagram of Figure 1.

3.4 $(-3, -2, -2, -3)$

In this subsection, we show the following proposition:

Proposition 20. *Every 3-manifold described by the graph in Figure 2 bounds a rational homology 4-ball.*

By Subsection 3.1, it is enough to show that the $(0, 0)$ surgery on the two-component unlink blows up to a $\mathbb{Z}_2$-equivariant image of the Kirby diagram of Figure 2 with two -1-framed 2-handles attached. By Proposition 17.4, one of the unknots with framing 0 blows up to the chain

$$(-\beta_{m_2}, \dots, -\beta_2, 1 - \beta_1, 1 - b_1, -b_2, \dots, -b_{m_1}),$$

which can be seen by noting that the above chain is one blow-up away from

$$(-\beta_{m_2}, \dots, -\beta_1, -1, -b_1, \dots, -b_{m_1}).$$

Our first move will be to link the other unknot with framing 0 to the component with framing $1 - \beta_1$ using a blow-up, thus obtaining Figure 15a. In this figure, the chains $(-b_2, \dots, -b_{m_1})$ and $(-\beta_2, \dots, b_{m_2})$ are represented by tiny squares that freely move on their respective components and if there are two on the same one, they could even pass through each other. Figure 15b is obtained from Figure 15a by a simple isotopy. Note that the purple -1-weighted component is linked with the black and the blue ones with negative clasps. We may thus use Figure 12c to blow it up into an arbitrary chain of negative clasps as in Figure 15c.

Now, zoom into the lower part of Figure 15c and note that it looks like Figure 16a. It is isotopic to Figure 16b, which clearly blows up to Figure 16c. This shows that Figure 15c blows up to Figure 17a. Applying an isotopy of the link gives Figure 17b. The green and the black components are now linked positively. The -1-blowup that gets rid of this linking introduces a new component that links to the green and the black components with a negative and positive clasp respectively. Repeated blow-ups thus give us a chain with all clasps negative except the lowest one. We conclude that Figure 17c is a $\mathbb{Z}_2$-equivariant blow-up of Figure 17b and hence of the $(0, 0)$ surgery on the 2-component unlink, but we may also note that removing the two -1-weighted components gives us a tree-shaped plumbing, namely the one in Figure 2.

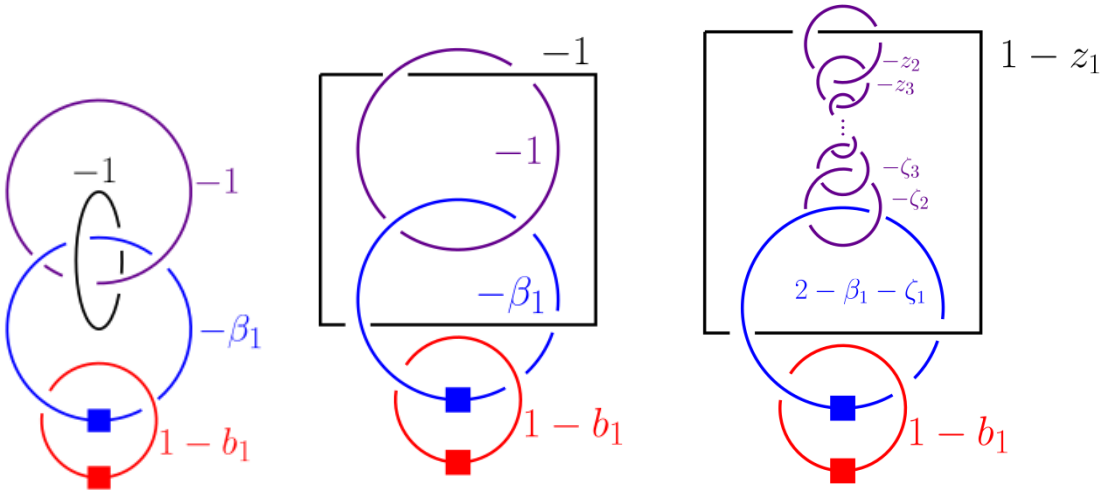

(a) (b) (c)

Figure 15: Creating a $\mathbb{Z}_2$-equivariant Kirby diagram of the Figure 2 with two extra 2-handles.

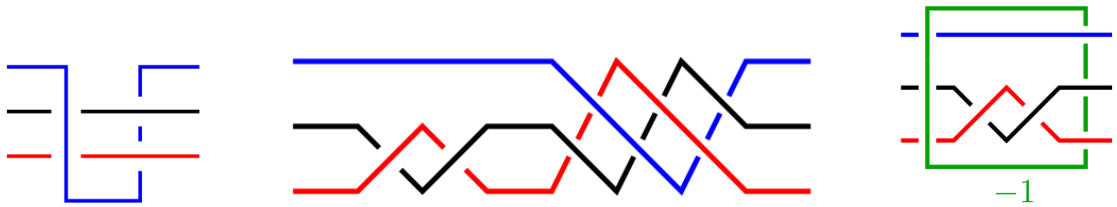

(a) (b) (c)

Figure 16: Zooming in on a part of Figure 15c and blowing up.

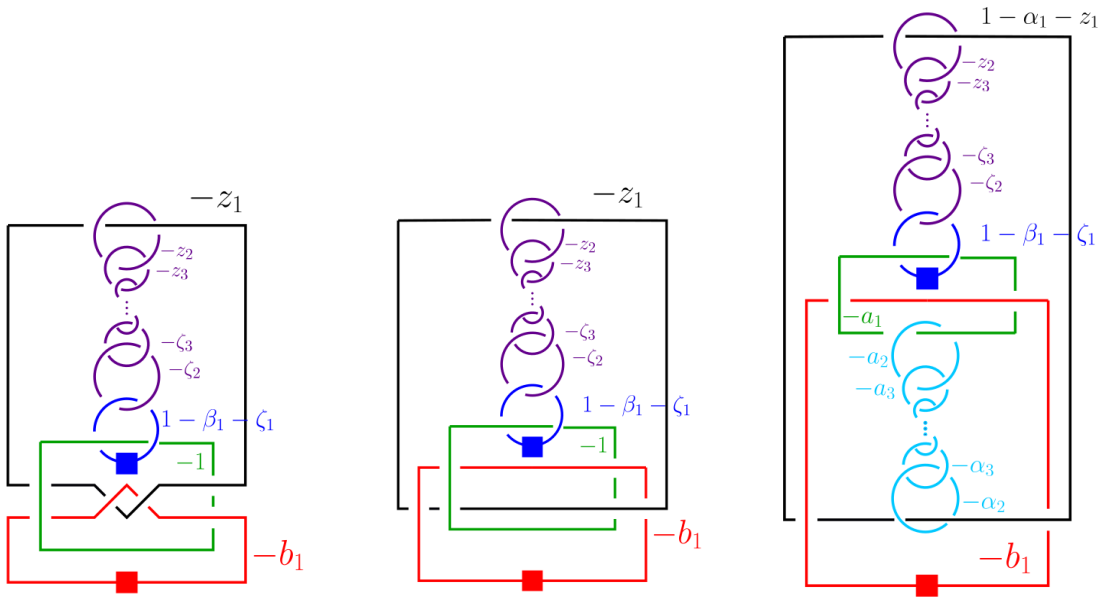

Figure 17: Creating a $\mathbb{Z}_2$-equivariant Kirby diagram of the Figure 2 with two extra 2-handles.

4 Proof of Theorem 5

In this section, we prove Theorems 5 and 6 by studying the intersection between the graphs in Figures 2, 1 and 3, and plumbing graphs of positive rational surgeries on positive torus knots. First we describe the plumbing graphs of the surgeries on torus knots, and then we go through the intersections with the graphs in Figures 2, 1 and 3 one by one. The change of order compared to Section 3 is because some families obtained from Figure 1 are subfamilies of families obtained from Figure 2.

4.1 Plumbing Graphs of Rational Surgeries on Torus Knots

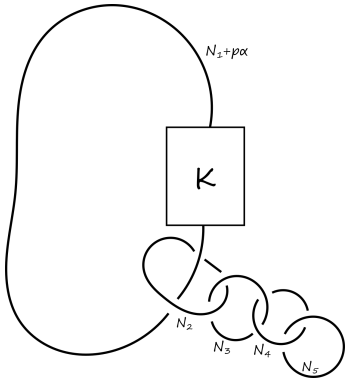

Figure 18: A Kirby diagram with boundary $S^3_n(T(p,\alpha))$ where $n = [N_1 + p\alpha, N_2, \ldots, N_k]^-$ and $K = T(p,\alpha)$, here drawn for $k = 5$.

In order to find the intersection between the plumbing graphs of rational surgeries on torus knots and the graphs obtained from Lisca's graphs by repeated GOCL and IGOCL moves, we need to know what the plumbing graphs of rational surgeries on torus knots look like. Let $n > 0$ be a rational number. We want to find a plumbing graph for $S^3_n(T(p,\alpha))$. We can write $n = [N_1 + p\alpha, N_2, \dots, N_k]^-$ for $N_2, \dots, N_k \geq 2$. The 3-manifold $S_n(T(p,\alpha))$ bounds the 4-manifold in Figure 18, which is positive-definite if $n > 0$. Now, we will use the same technique as in [18, Section 3] in order to produce a definite plumbing graph. In the process, we need to measure how far we are from being definite, so the following definition is useful.

Definition 21. *The **positive/negative index** of a 4-manifold is the number of positive/negative eigenvalues of its intersection form.*

The argument of [18, Section 3] that the blow-ups decrease the surgery coefficient by a constant still holds to show that $S^3_n(T(p,\alpha))$ bounds the 3-manifold described by the graph in Figure 19.

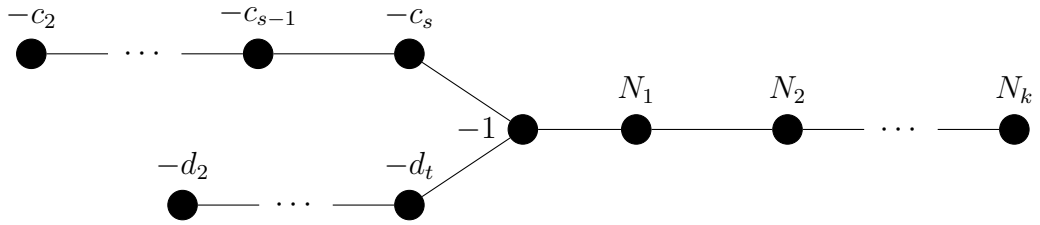

Figure 19: A plumbing graph of $S^3_n(T(p,\alpha))$, where $\alpha > p$. Here $[1, c_2, ..., c_s]^- = p/\alpha$, $[d_1, \dots, d_t]^- = \alpha/p$ and $[N_1, \dots, N_k]^- = N = n - p\alpha$. In particular, the pair of fractions $([c_2, \dots, c_s]^-, [d_1, \dots, d_t]^-)$ are complementary. Also, we can write $[(c_2, c_3, \dots, c_s) = (-2^{[d_1-2]}, a_1 + 1, a_2, \dots, a_r)$ so that $[a_1, \dots, a_r]^-$ and $[d_2, \dots, d_t]^-$ are complementary.

The positive index of this graph is k by the same logic as in [18, Section 3]. To obtain a definite graph, we will need the following generalisation of the algorithm in [18, Figure 2]:

Proposition 22. *Let Γ be a tree-shaped chain graph containing a chain (a connected linear subgraph with no nodes, that is vertices of degree greater than 2) $(-\alpha_1, \dots, -\alpha_k)$, as in Figure 20a. Let Γ' be the graph Γ with the chain substituted by the chain $(\beta_1, \dots, \beta_j)$, for $[\alpha_1, \dots, \alpha_k]^-$ and $[\beta_1, \dots, \beta_j]^-$ complementary fractions, and the weight of the vertices adjacent to the chain increased by 1. Then $Y_\Gamma = Y_{\Gamma'}$. Moreover, $b^2_+(X_{\Gamma'}) = b^2_+(X_\Gamma) + j$ and $b^2_-(X_{\Gamma'}) = b^2_-(X_\Gamma) - k$.*

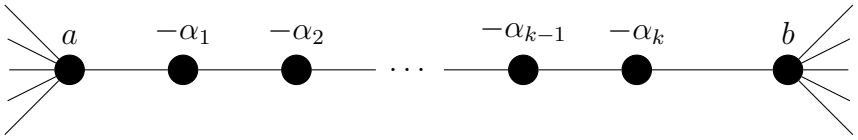

(a) Changing a negative chain...

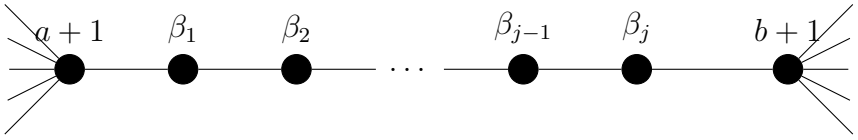

(b) ... to a positive one.

Figure 20: The graphs above bound the same 3-manifold if $[\alpha_1, \ldots, \alpha_k]^-$ and $[\beta_1, \ldots, \beta_j]^-$ are complementary fractions.

Example. Before sketching the proof, we will provide an example of the algorithm that we use to change such a chain. Start with the linear graph $(-2, -4, -2)$. Right now, all vertices have negative weights. We want to introduce a positively weighted vertex. Let us perform a 1-blow-up. We obtain $(1, -1, -4, -2)$. Now, we blow down the -1 and obtain $(2, -3, -2)$. We perform a 1-blow-up between the 2 and the -3 and obtain $(3, 1, -2, -2)$. Blowing up a 1 again between the last positively weighted vertex and the first negatively weighted one gives us $(3, 2, 1, -1, -2)$. We blow down the -1 to get $(3, 2, 2, -1)$ and again to obtain $(3, 2, 3)$. We note that every time we perform a 1-blow-up, we increase both the positive index and the number of positive vertices by 1, and every time we perform a -1-blowdown, we decrease both the negative index and the number of negative vertices by 1. Thus, changing these 3 negative vertices into 3 positive ones decreased the negative index by by 3 and increased the positive index by 3.

Proof sketch. This proposition follows from the fact that blow-ups and blow-downs do not change the boundary 3-manifold, together with the algorithm of 1) performing a 1-blow-up at the right of the rightmost chain element greater than 1, 2) blowing down any -1-weighted vertices, and 3) repeating. Following the Riemenschneider diagram, we see that this algorithm gradually substitutes a sequence by its Riemenschneider dual. Blowing up by 1 increases both the positive index and the number of vertices with positive weight by 1, and blowing down a -1 decreases both the number of vertices with negative weight and the negative index by 1. Thus, substituting the k negative-weighted vertices by j positive-weighted ones substracts k from the negative index and adds j to the positive index. □

If $N > 1$ and thus $N_1 \geq 2$, we can use Proposition 22 to substitute the chain $(N_1, \ldots, N_k)$ with its negative Riemenschneider complement $(-M_1, \ldots, -M_j)$ and obtain the negative-definite graph in Figure 21.

If $0 < N < 1$, then the sequence $(N_1, \ldots, N_k)$ starts with a 1 possibly followed by some 2's that we can blow down before turning the rest of the chain negative. This will once again give us a negative-definite graph, namely the one in Figure 22.

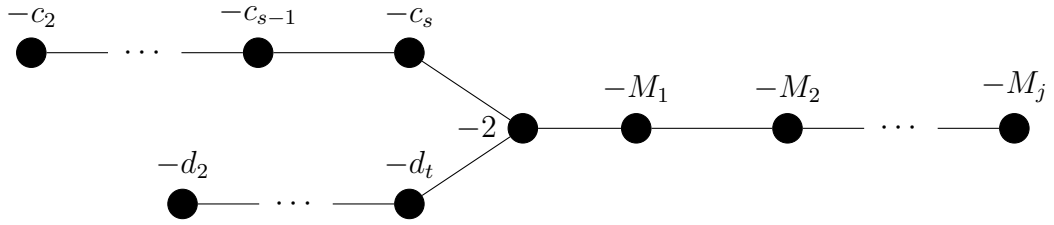

Figure 21: A negative-definite plumbing graph of $S^3_n(T(p,\alpha))$, where $N = n - p\alpha > 1$ and $\alpha > p$. Here $[1, c_2, ..., c_s]^- = p/\alpha$, $[d_1, \ldots, d_t]^- = \alpha/p$ and if $N = n - p\alpha = a/b$ with $a, b \in \mathbb{Z}_{>0}$, then $[M_1, \ldots, M_j]^- = \frac{a}{a-b}$.

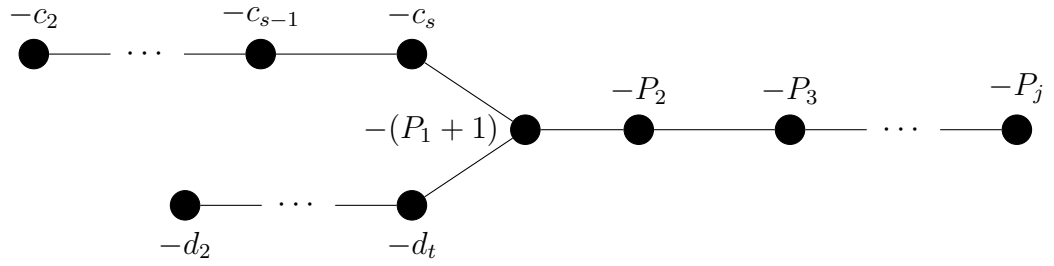

Figure 22: A negative-definite plumbing graph of $S^3_n(T(p,\alpha))$, where $\alpha > p$ and $0 < n - p\alpha = N < 1$. Here $[1, c_2, ..., c_s]^- = p/\alpha$, $[d_1, \ldots, d_t]^- = \alpha/p$ and the fraction $[P_1, \ldots, P_j]^-$ is complementary to $\frac{1}{1-N} = [N_2, \ldots, N_k]^-$. In fact, that means that $N = \frac{1}{[P_1,\ldots,P_j]^-}$.

If $N < 0$, that is $N_1 \leq 0$, then changing turning the positively-weighted vertices $(N_2, \ldots, N_k)$ negative will not be enough to decrease the positive index to 0. Instead, we will use Proposition 22 to turn the two other legs of our graph positive, and we obtain the graph in Figure 23, which has negative index 1.

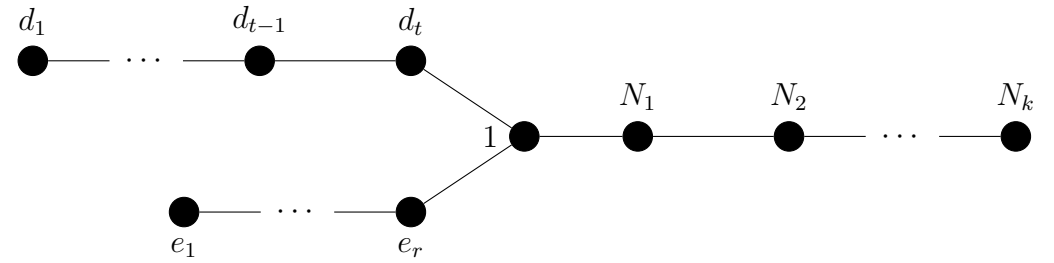

Figure 23: A plumbing graph of $S^3_n(T(p,\alpha))$, where $\alpha > p$ and $n - p\alpha = N < 0$. Here the negative index is 1, $[d_1, \ldots, d_t]^- = \alpha/p$ and $[e_1, \ldots, e_r]^-$ is complementary to $[d_2, \ldots, d_t]^-$.

If $N_1 = 0$, we will perform a 0-absorption (see [20, Proposition 1.1]) and obtain the positive definite graph in Figure 24.

If $N_1 = -1$, we simply blow it down. If $N_1 \leq 2$, we use Proposition 22 to turn it into a chain of 2's and obtain the graph in Figure 25.

In the graphs of Figures 21 22, 24 and 25, the vertex of degree 3 is called the

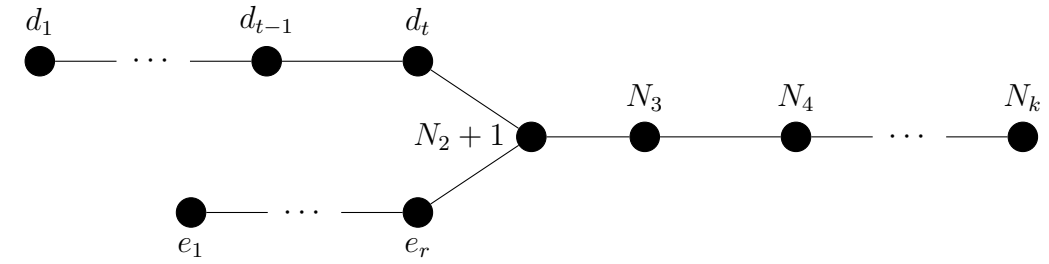

Figure 24: A positive definite plumbing graph of $S^3_n(T(p,\alpha))$, where $\alpha > p$ and $-1 < N = n - p\alpha < 0$. Here $[d_1,\dots,d_t]^- = \alpha/p$ and $[e_1,\dots,e_r]^-$ is complementary to $[d_2,\dots,d_t]^-$.

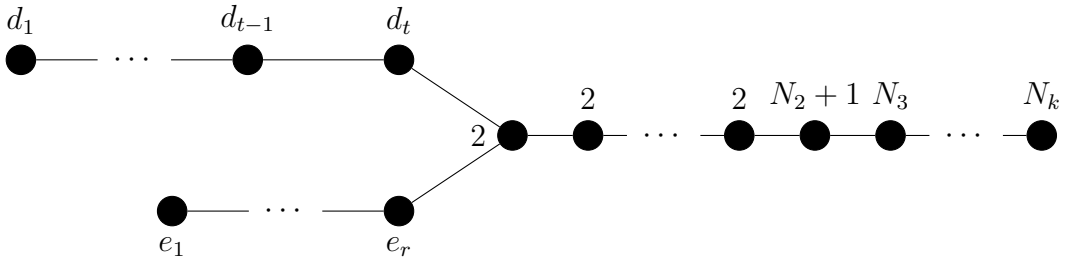

Figure 25: A positive definite plumbing graph of $S^3_n(T(p,\alpha))$, where $\alpha > p$ and $n - p\alpha = N < -1$. Here $[d_1,\dots,d_t]^- = \alpha/p$ and $[e_1,\dots,e_r]^-$ is complementary to $[d_2,\dots,d_t]^-$, and the tail starts with a chain of -2's of length $-N_1 - 1$.

node. Removing the node splits the graph into 3 connected components, of which the top left one is called the *torso*, the bottom left one is called the *leg* and the right one is called the *tail*. This vocabulary is chosen to accord with the vocabulary of [18] on iterated torus knots. We also often talk about the torso, leg and tail collectively as legs. This comes from viewing the graphs as general star-shaped graphs rather than graphs of surgeries on torus knots specifically. (The author recommends looking at a flag of Sicily or Isle of Man for a more precise metaphor.) This vocabulary is generally used by Lecuona, for instance in [14] and [15].

We say that two legs of a star-shaped graph are negatively quasi-complementary if either adding one vertex at the end of one leg could make them complementary, and positively quasi-complementary if removing a final vertex from one of the legs could. We say that two legs are complementary if they are either positively or negatively quasi-complementary. Note that the graphs in Figures 21, 22, 24 and 25 are exactly the star-shaped graphs with three legs whereof two are quasi-complementary. In the following subsections, we are thus going to look for star-shaped graphs with a pair of quasi-complementary legs among the graphs in Figures 3, 2 and 1. The following very easy-to-check proposition will come in useful:

Proposition 23. *Suppose $Q/P = [a_1,\dots,a_n]^-$ and $(-a_1,-a_2,\dots,-a_n)$ is either the leg or torso of the plumbing graph of $S^3_r(T(p,\alpha))$, a positive rational surgery on a positive torus knot. (Here $-a_n$ is the weight of the vertex adjacent to the node.) Then α/p is one of the following:*

- $\frac{Q}{P}$,

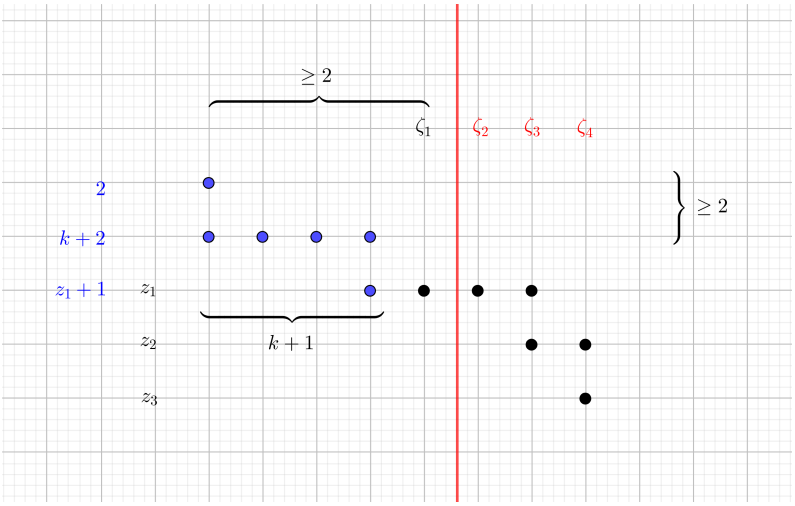

Figure 26: It is impossible to choose k so that the length or height difference between the full Riemenshneider diagram and the diagram to the right of the red line is one.

- $\frac{Q}{Q-P}$,
- $\frac{(l+1)Q+P}{Q}$ *for some* $l \geq 0$ *or*
- $\frac{(l+2)Q-P}{Q}$ *for some* $l \geq 0$.

Note that if $\mathrm{GCD}(P,Q) = 1$, then all of these fractions are reduced. However, if $P = Q-1$, then, $\alpha/p = \frac{Q}{Q-P} = Q$ is a degenerate case that we ignore.

4.2 $(-3,-2,-2,-3)$

In this subsection, we prove the following:

Proposition 24. *For all torus knots $T(p,q)$ in Families 1, 2, 3, 4, 6 and 7 of Theorem 5, there exists an $r \in \mathbb{Q}_+$ such that $S^3_r(T(p,q))$ bounds a rational homology ball.*

This is done by considering the intersections between the graphs in Figures 21, 22, 24 and 25 (rational surgeries on torus knots) and the graphs in Figure 2 (graphs obtainable from $(-3,-2,-2,-3)$ through GOCL moves).

Proof. Figure 2 is symmetric in the y-axis, so it is enough to try two of the vertices for trivalency, say the one with weight $1-\beta_1-\zeta_1$ and the one with weight $-a_1$.

If we want to the vertex with weight $1-\beta_1-\zeta_1$ to be the trivalent vertex in one of the Figures 21, 22, 24 and 25 , then $l_1 = m_1 = 1$. Hence $\beta_i = \alpha_j = 2$ for all i and j. Also, $l_2 = 1$ or $n_1 = 1$. Suppose that $(-\beta_{m_2},\dots,-\beta_2)$ is one of the quasi-complementary legs. Proposition 23 would generate that (p,q) belongs to Families 1 and 2 in Theorem 5. All of these are possible to produce by setting $l_2 = 1$, which frees us up to choosing $(\zeta_2,\cdots,\zeta_{n_2})$ completely freely.

Now, we consider what happens if the legs other than $(-\beta_2,\dots,-b_{m_2})$ are quasi-complementary. If $n_1 = 1$, all αs, βs and ζs become -2, giving us a star-shaped

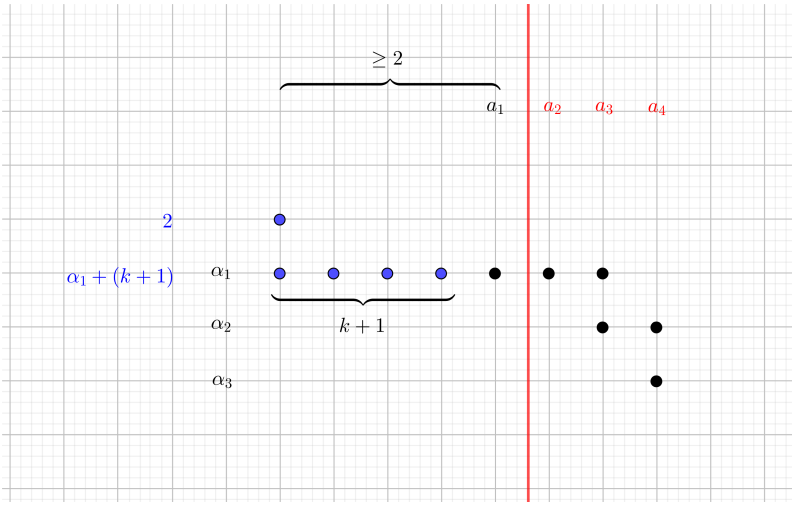

Figure 27: Riemenschneider diagram of the quasi-complementary legs $(-a_2, \ldots, -a_{l_1})$ and $(-b_1, 1-\alpha_1-z_1, -\alpha_2, \ldots, -\alpha_{l_2})$ in Figure 2 when $m_1 = n_1 = m_2 = 1$.

graph with two legs containing nothing but -2s, not allowing us out of the families 1, 2, 3 and 4. We consider the case $l_2 = 1$ instead. We have $a_1 = \alpha_1 = 2$. Let $b_1 = k+2$ (so that the leg $(-\beta_2, \ldots, -\beta_{m_2}) = (-2, \ldots, -2)$ has length k). We investigate if $(-\zeta_2, \ldots, -\zeta_{n_2})$ and $(-2, -(k+2), -z_1-1, -z_2, \ldots, -z_{n_1})$ can be quasi-complementary. Consider the diagram in Figure 26. The black dots represent the Riemenschneider diagram of $(z_1, \ldots, z_{n_1})$ and $(\zeta_1, \ldots, \zeta_{n_2})$. The blue dots are added in such a way that they together with the black dots form the Riemenschneider diagram of $(-2, -(k+2), -z_1-1, -z_2, \ldots, -z_{n_1})$. Call it the BB diagram. The Riemenschneider diagram of $(-\zeta_2, \ldots, -\zeta_{n_2})$ is to the right of the red line. Call it the RR diagram. Now we wonder if we can choose the black dots and k in such a way that the BB diagram is just the RR diagram plus one row or column at the end. However, we see that it is impossible to create a difference of one between the length of one leg and the complement of the other leg.

Now, consider the vertex labelled $-a_1$ being trivalent instead. This means that $m_1 = 1$. Also, either $n_1 = 1$ or $l_2 = 1$. First, assume that $n_1 = 1$. This means that $\beta_1 = \cdots = \beta_{m_2} = \zeta_1 = \cdots = \zeta_{n_2} = 2$. Either n_2 or m_2 must be 1. No matter the choice, the left leg becomes $(-2, \ldots, -2, -3)$ from the outside. If it is included in a pair of quasi-complementary legs, which we can always ensure since we can choose $(\alpha_2, \ldots, \alpha_{l_1})$ freely, we can use Proposition 23 to get all of families 3 and 4. In the more interesting case (where the leftmost leg is not one of the quasi-complementary ones) $(a_2, \ldots, a_{l_1})$ must be quasi-complementary (from the inside) either to $(2, 1+k+\alpha_1, \ldots, \alpha_{l_2})$ for some $k \geq 0$ (depicted in Figure 27) or to $(2+k, 1+\alpha_1, \ldots, \alpha_{l_2})$ for some $k \geq 0$ (depicted in Figure 28), depending on whether n_2 or m_2 is equal to 1.

Let us resolve the first case. Again, in order for $(a_2, \ldots, a_{l_1})$ to be quasi-complementary to $(2, 1+k+\alpha_1, \ldots, \alpha_{l_2})$ for some $k \geq 0$, the BB diagram should be the same as the RR diagram plus an extra row or column at the end. Since the part to the left of the red line has at least two columns, it must be an extra row. One

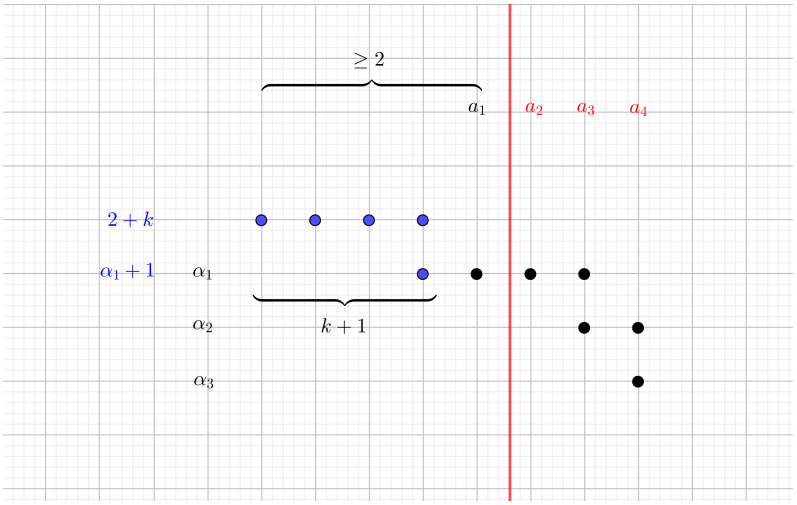

Figure 28: Riemenschneider diagram of the quasi-complementary legs $(-a_2, \ldots, -a_{l_1})$ and $(-b_1, 1-\alpha_1-z_1, -\alpha_2, \ldots, -\alpha_{l_2})$ in Figure 2 when $m_1 = n_1 = n_2 = 1$.

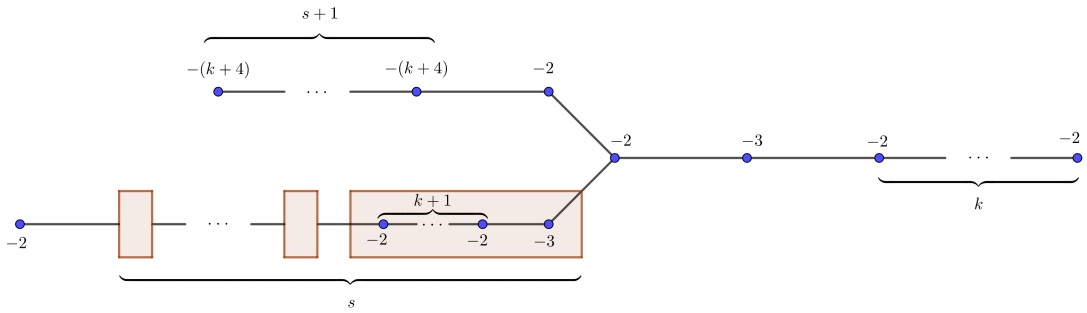

Figure 29: A strange two-parameter family of rational surgeries on positive torus knot that bound rational homology 4-balls.

solution would be $(\alpha_1, \dots, \alpha_{l_2}) = (3)$. If the black diagram has more than one row, we need $\alpha_2 = (k+1)+2+1 = k+4$. We can add as many rows as we want this way. We get that $(\alpha_1, \dots, \alpha_{l_2}) = (3, (k+4)^{[s]})$ and $(a_1, \dots, a_{l_1}) = (2, (3, (2)^{[k+1]})^{[s]}, 2)$, giving us the graph in Figure 29. This graph is of the shape of Figure 25, so it describes $S^3_n(T(p,\alpha))$ for $\alpha/p = [(k+4)^{[s+1]}, 2]^-$ and $N = n - p\alpha = [-1, (2)^{[k+1]}]^- = -\frac{2k+3}{k+2}$. This corresponds to family 6 in Theorem 5. A different formulation of the result is that $S^3_{p\alpha - \frac{2k+3}{k+2}}(T(p,\alpha))$ bounds a rational homology ball for all p and α described by

$$\begin{pmatrix} \alpha \\ p \end{pmatrix} = \begin{pmatrix} k+4 & -1 \\ 1 & 0 \end{pmatrix}^{s+1} \begin{pmatrix} 2 \\ 1 \end{pmatrix}$$

for some $s, k \geq 0$. This two-parameter family is the most spectacular one we've seen to date since it is polynomial in one variable and exponential in the other.

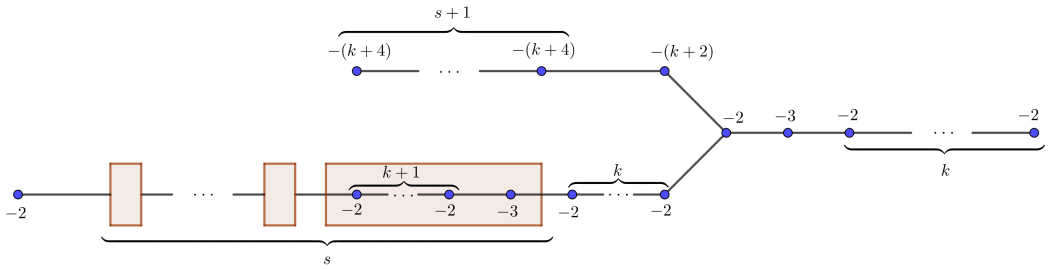

Figure 30: A strange two-parameter family of rational surgeries on positive torus knot that bound rational homology 4-balls.

In the second case, that is if $(a_2, \dots, a_{l_1})$ is quasi-complementary to $(2+k, 1+\alpha_1, \dots, \alpha_{l_2})$ for some $k \geq 0$, then $(\alpha_1, \dots, \alpha_{l_2}) = (k+3, (k+4)^{[s]})$ for some $s \geq 0$. Then the graph becomes as in Figure 30. Now $\alpha/p = [(k+4)^{[s+1]}, k+2]^-$, meaning that $S^3_{p\alpha - \frac{2k+3}{k+2}}(T(p,\alpha))$ bounds a rational homology ball for all p and α described by

$$\begin{pmatrix} \alpha \\ p \end{pmatrix} = \begin{pmatrix} k+4 & -1 \\ 1 & 0 \end{pmatrix}^{s+1} \begin{pmatrix} k+2 \\ 1 \end{pmatrix}$$

for some $s, k \geq 0$. This family is similarly spectacular to the previous one. It corresponds to Family 7 in Theorem 5.

If $l_2 = 1$ instead of $n_1 = 1$, then $a_1 = \dots = a_{l_1} = 2$. We already know that we can choose surgery coefficients when one of the complementary legs consists of only -2s, so we do not need to check that case to formulate Theorem 5. In fact we do not need to check further, as any star-shaped graphs with three legs whereof two are quasi-complementary, the third one consisting only of -2s and the node having weight -2 is a positive integral surgery on a positive torus knot, which have been classified in [3]. □

4.3 $(-3, -2, -3, -3, -3)$

In this subsection, we prove the following:

Proposition 25. *For all torus knots $T(p,q)$ in the families 5 and 11 of Theorem 5, there exists an $r \in \mathbb{Q}$ such that $S^3_r(T(p,q))$ bounds a rational homology ball.*

This is done by finding the intersections between the graphs in Figures 21, 22, 24 and 25 (rational surgeries on torus knots) and the graphs in Figure 1 (graphs obtainable from $(-3,-2,-3,-3,-3)$ through GOCL and IGOCL moves).

Proof. In Figure 1 there are three possibilities for a trivalent vertex. If we choose the vertex of weight $-a_1$, then $m_2 = 1$ and thus two of the legs are $(-3-k)$ and $(-2,\dots,-2)$. We already know that if one of these is in a quasi-complementary pair, then (p,α) lies in families 1-4 in Theorem 5, so we get nothing new. Choosing the vertex of weight $-(1+b_1)$ to be trivalent, and noting that we land in families 1-4 if the left leg $(-3-k,-2)$ is one of the quasi-complementary ones, does however lead us to find that

$$S^3_{p\alpha-\frac{5}{7}}(T(p,\alpha))$$

bounds a rational homology ball for every

$$\begin{pmatrix}\alpha\\ p\end{pmatrix} = \begin{pmatrix}5 & -1\\ 1 & 0\end{pmatrix}^{s+1}\begin{pmatrix}3\\ 1\end{pmatrix}$$

where $s \geq 0$. This corresponds to family 8 in Theorem 5. Finally, choosing the vertex of weight $-(1+\alpha_1)$ to be trivalent gives us $m_1 = n_1 = 1$. If the lower leg $(-2,\dots,-2)$ is included in the pair of quasi-complementary legs, we fall into families 1-4 again. We need to investigate when $(-(3+k),-a_1,-(1+b_1))$ can be quasi-complementary to $((-2)^{[b_1-2]},-3,(-2)^{[k]})$. The Riemenschneider dual of the latter leg is $(-b_1,-(k+2))$, so we need $b_1 = a_1$ and $k+2 = b_1+1$. Note that we also need $a_1 \geq 3$ in order to get a three-legged graph. Let $a = a_1 - 3$. We get $(-(3+k),-a_1,-(1+b_1)) = (-(a+5),-(a+3),-(a+4))$. Our graph is now as in Figure 24. Thus $\alpha/p = [a+5,a+3,a+4]^- = \frac{a^3+12a^2+45a+51}{a^2+7a+11}$. This correspond to family 5 in Theorem 5. □

The remaining families follow from [15] and [3].

4.4 $(-2,-2,-3,-4)$

In this subsection, we prove Theorem 6.

This is done by determining the intersection between the graphs in Figures 21, 22, 24 and 25 and the graphs in Figure 3, that is between the graphs of surgeries on torus knots and the graphs of Figure 3, which we now know to bound rational homology balls.

Proof of Theorem 6. To turn Figure 3 into a star-shaped graph, we will need to keep some of the grown complementary legs to length 1. If we let the vertex of weight $-1-a_1$ be trivalent, then $m_1 = 1$ and thus $(\beta_1,\dots,\beta_{m_2})$ consists only of 2's. If $m_2 > 1$ then $n_2 = 1$ and $(a_1,\dots,a_{n_1}) = (2,\dots,2)$. In order to have trivalency of the $-(1+a_1)$ vertex, $\alpha_1 \geq 3$ is required. It is easy to check that in this case the only legs that can be quasi-complementary are the $(-b_1,-(2+k))$ one and the $(\underbrace{-2,\dots,-2}_{\alpha_1-2})$

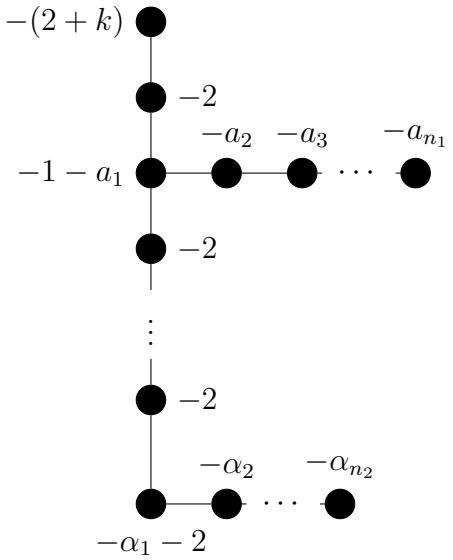

Figure 31: Choosing $m_1 = m_2 = 1$ in Figure 3 gives this star-shaped graph.

one. They can either be negatively quasi-complementary, made complementary by adding -3 at the end of the second leg, in which case $\alpha_1 = b_1$ and $k = 0$ have to hold, or they can be positively quasi-complementary, made complementary by removing $-(2+k)$ from the first one, in which case $\alpha_1 - 2 = b_1 - 1$. The first case shows that

$$S^3_{\frac{(2b_1^2-2b_1+1)^2}{2b_1^2-b_1+1}}(T(b_1-1, 2b_1-1))$$

bounds a rational homology ball for any $b_1 \geq 3$. The second case shows that

$$S^3_{\frac{((k+2)b_1^2-1)^2}{(k+2)b_1^2+b_1-1}}(T(b_1, b_1(k+2)-1))$$

bounds a rational homology ball for all integers $b_1 \geq 2$ and $k \geq 0$. Both of these are subfamilies to families 1 and 2 in Theorem 5 that we will show can in fact be fully realised.

We get more interesting families when we let $m_2 = 1$, because then $(\alpha_1, \ldots, \alpha_{n_2})$ can be anything as long as it has something but a 2 somewhere so that $n_1 > 1$. We will get graphs of the form in Figure 31. To make the top and right legs quasi-complementary is easy: we need to choose whether they are to be positively or negatively quasi-complementary and which leg needs an extra vertex or a vertex removed to be complementary, and then we just need to choose $(a_2, \ldots, a_{n_1})$ that make it happen. We use Proposition 23 for $Q/P = [2+k, 2]^- = \frac{2k+3}{2}$. This corresponds to the entire families 3 and 4 as well as subfamilies of families 1 and 2 in Theorem 5. The top and bottom legs cannot be made quasi-complementary.

The most interesting case to consider is whether the right and the bottom legs can be made quasi-complementary. In Figure 32, the black dots show a Riemenschneider diagram of the complementary sequences $(a_1, \ldots, a_{n_1})$ and $(\alpha_1, \ldots, \alpha_{n_2})$. Adding the blue dots gives us a Riemenschneider diagram for the sequence $(\underbrace{2, \ldots, 2}_{k}, \alpha_1 +$

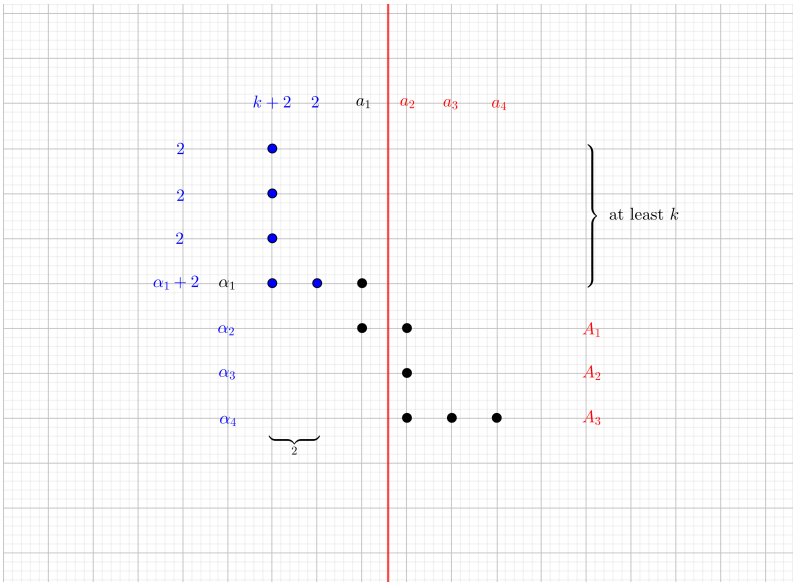

Figure 32

$2, \alpha_2, \ldots, \alpha_{n_2}$) (with complement $(k+2, 2, a_1, \ldots, a_{n_1})$). Considering only the part to the right of the red line gives us a Riemenschneider diagram for $(a_2, \ldots, a_{n_1})$ (with a complement $(A_1, \ldots, A_{n_3})$). In order for $(\underbrace{2, \ldots, 2}_{k}, \alpha_1+2, \alpha_2, \ldots, \alpha_{n_2})$ and $(a_2, \ldots, a_{n_1})$ to be quasi-complementary, either the picture to the right of the red line and the total picture without the last line, or the total picture and the picture to the right of the the red line with an extra column, must be the same. The sequences $(k+2, 2, a_1, \ldots, a_{n_1})$ and $(a_2, \ldots, a_{n_1})$ have length difference 2, removing the second option. The only ways in which $(\underbrace{2, \ldots, 2}_{k}, \alpha_1+2, \alpha_2, \ldots, \alpha_{n_2})$ and $(A_1, \ldots, A_{n_3})$ can have length difference 1 is if any of the following hold:

1. $k = 0$ and $a_1 = 3$, or
2. $k = 1$ and $a_1 = 2$.

If $k = 0$ and $a_1 = 3$, then the first row of the total picture has length 3. Thus, in the second total row, to the right of the red line, we need three dots, making a total of 4 dots. This is a valid solution, namely $(\alpha_1, \ldots, \alpha_{n_2}) = (2, 5)$, $(\alpha_1+2, \alpha_2, \ldots, \alpha_{n_2}) = (4, 5)$, $(A_1, \ldots, A_{n_3}) = (4)$ and $(a_1, \ldots, a_{n_1}) = (3, 2, 2, 2)$. If we choose to continue and add α_3, that means adding a new row completely to the right of the red line, which must be as long as the second total row, namely 4 dots. That again gives a valid solution $(\alpha_1, \ldots, \alpha_{n_2}) = (2, 5, 5)$, $(\alpha_1+2, \alpha_2, \ldots, \alpha_{n_2}) = (4, 5, 5)$, $(A_1, \ldots, A_{n_3}) = (4, 5)$ and $(a_1, \ldots, a_{n_1}) = (3, 2, 2, 3, 2, 2, 2)$. We can continue this process and obtain the solution $(\alpha_1, \ldots, \alpha_{n_2}) = (2, (5)^{[l]})$ and $(a_1, \ldots, a_{n_1}) = ((3, 2, 2)^{[l]}, 2, 2)$ for all $l \geq 1$. Our legs are positively quasi-complementary, so $\alpha/p = [d_1, \ldots, d_t]^- = [(5)^{[l]}, 4]^-$. Since $5 - \frac{b}{a} = \frac{5a-b}{a}$, we have that

$$\begin{pmatrix} \alpha \\ p \end{pmatrix} = \begin{pmatrix} 5 & -1 \\ 1 & 0 \end{pmatrix}^l \begin{pmatrix} 4 \\ 1 \end{pmatrix}$$

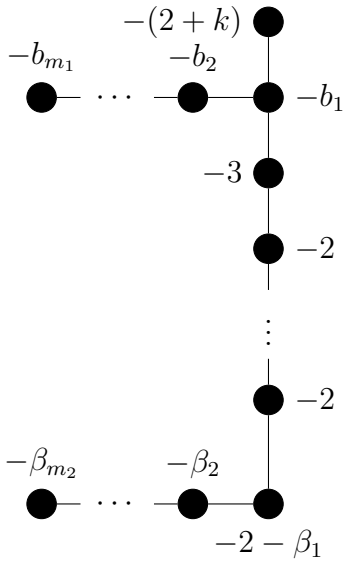

Figure 33: Choosing $n_1 = n_2 = 1$ in Figure 3 gives this star-shaped graph.

for $l \geq 1$. This corresponds to family 6 in Theorem 5. We can compute $N = [0,3,2,2]^- = -\frac{3}{7}$. In other words, if $p_1 = 1$, $p_2 = 4$ and $p_{j+2} = 5p_{j+1} - p_j$ for all $j \geq 0$ [21, A004253], we can say that

$$S^3_{p_j p_{j+1} - \frac{3}{7}}(T(p_j, p_{j+1}))$$

bounds a rational homology ball for all $j \geq 1$. In this form it may not be obvious that the numerator of the surgery coefficient is a square, but in fact, $p_j p_{j+1} - \frac{3}{7} = \frac{V_{j+1}^2}{7}$ for V_j being a sequence defined by $V_1 = 2$, $V_2 = 5$ and $V_{j+2} = 5V_{j+1} - V_j$ for all $j \geq 0$ [21, A003501]. It is a shifted so called Lucas sequence. The equality can be proven by first proving by induction that $p_{j+2}p_j - p_{j+1}^2 = 3$ for all $j \geq 0$, then noting that $V_{j+1} = p_{j+1} + p_j$ for all $j \geq 0$, and finally combining these equalities.

If $k = 1$ and $a_1 = 2$ the argument goes the same way. The only way for the right and bottom legs to be quasi-complementary is if the Riemenschneider diagram to the right of the red line and the total diagram missing the bottom line coincide. By the same argument as above, it happens if and only if $(\alpha_1, \ldots, \alpha_{n_2}) = (3, (5)^{[l]})$ and $(a_1, \ldots, a_{n_1}) = (2, (3,2,2)^{[l]}, 2)$ for all $l \geq 0$. In this case $\alpha/p = [(5)^{[l]}, 5, 2]^-$ and $N = [0,2,2,3]^- = -\frac{5}{7}$. This shows that if $Q_1 = 2$, $Q_2 = 9$ and $Q_{j+2} = 5Q_{j+1} - Q_j$ for all $j \geq 1$, then

$$S^3_{Q_j Q_{j+1} - \frac{5}{7}}(T(Q_j, Q_{j+1}))$$

bounds a rational homology ball for all $j \geq 1$. This corresponds to family 7 in Theorem 5. Just as before, we can show that

$$Q_j Q_{j+1} - \frac{5}{7} = \frac{(Q_j + Q_{j+1})^2}{7}.$$

Returning to Figure 3, we can let the vertex of weight $-b_1$ be the only node. That forces $n_1 = 1$, so $(\alpha_1, \ldots, \alpha_{n_2}) = (2, \ldots, 2)$. Putting $a_1 = 2$ would give us complete freedom in choosing $(b_2, \ldots, b_{m_1})$, so Proposition 23 applied to $Q/P =$

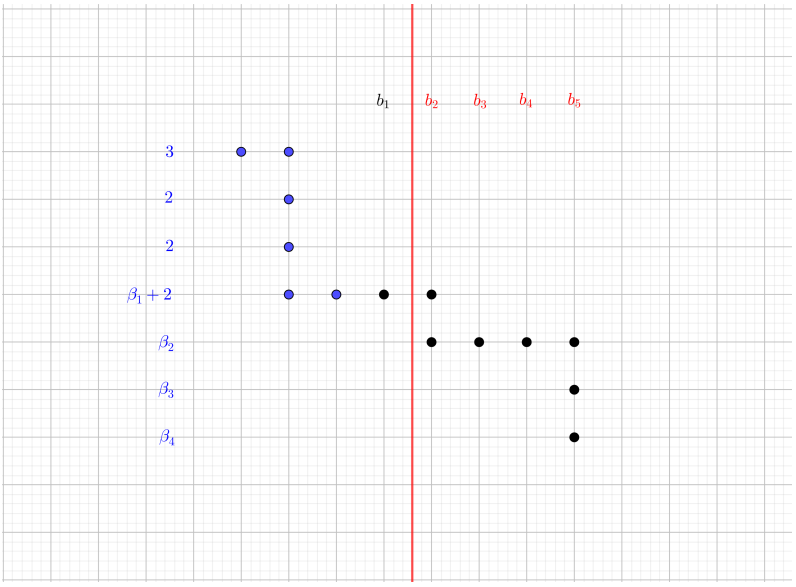

Figure 34

$2+k$ gives that there are surgery coefficients n such that $S^3_n(T(k+1,k+2))$, $S^3_n(T(k+2,(l+2)(k+2)-1))$ and $S^3_n(T(k+2,(l+1)(k+2)+1))$ bound rational homology 4-balls. These families correspond to the entire families 1 and 2 in Theorem 5. (Note however, that a couple of subfamilies of these will also be realised if we choose $a_1 > 2$ because $(b_2,\dots,b_{m_1}) = (2,\dots,2)$. These subfamilies have an especially ample supply of choices of surgery coefficents.) If $n_2 > 1$, then $m_2 = 1$ and $(b_1,\dots,b_{m_1}) = (2,\dots,2)$. We will have three legs, namely $(-(2+k))$, $((-2)^{[\beta_1-2]})$ and $(-(1+a_1),(-2)^{[k]},-(2+\beta_1),(-2)^{[a_1-2]})$. The first two can be quasi-complementary in two ways, but the generated pairs (p,α) are already known. The first and the third cannot be quasi-complimentary. The last two can also not be quasi-complementary if $n_2 > 1$. It is once again more interesting if $n_2 = 1$ and $m_2 > 1$ is allowed. We get the graph in Figure 33. The top and the bottom legs cannot be made quasi-complementary. The left and the bottom legs are the interesting case. Analogously to how we used Figure 32, we can use Figure 34 to show that $k = 0$ and $(\beta_1,\dots,\beta_{m_2}) = (4,(6)^{[l]})$ and $(b_1,\dots,b_{m_1}) = (2,2,(3,2,2,2)^{[l]},2)$. This is in fact family (4) in [3, Theorem 1.1] and family 8 in Theorem 5.

Going back to Figure 3, we could also make the vertex of weight $-\alpha_1-\beta_1$ the only trivalent vertex, but that would require $m_1 = n_1 = 1$ and thus all α_i and all a_j are 2's. The top leg would not be able to be quasi-complementary to a sequence of 2s, and the only way for the left and right legs to be quasi-complementary is if they are the legs (-2) and $(-2,-2)$ in either order. This just gives us two new families of possible surgery coefficients on $T(2,3)$. □

References

[1] Paolo Aceto. "Rational homology cobordisms of plumbed manifolds". In: *Algebr. Geom. Topol.* 20.3 (2020), pp. 1073–1126. ISSN: 1472-2747. DOI: 10.

2140/agt.2020.20.1073. URL: https://doi-org.ezproxy.lib.gla.ac.uk/10.2140/agt.2020.20.1073.

[2] Paolo Aceto and Marco Golla. "Dehn surgeries and rational homology balls". In: *Algebr. Geom. Topol.* 17.1 (2017), pp. 487–527. ISSN: 1472-2747. DOI: 10.2140/agt.2017.17.487. URL: https://doi-org.ezproxy.lib.gla.ac.uk/10.2140/agt.2017.17.487.

[3] Paolo Aceto, Marco Golla, Kyle Larson and Ana G. Lecuona. "Surgeries on torus knots, rational balls, and cabling". In: *arXiv e-prints*, arXiv:2008.06760 (Aug. 2020), arXiv:2008.06760. arXiv: 2008.06760 [math.GT].

[4] Selman Akbulut and Kyle Larson. "Brieskorn spheres bounding rational balls". In: *Proc. Amer. Math. Soc.* 146.4 (2018), pp. 1817–1824. ISSN: 0002-9939.

[5] Kenneth L. Baker, Dorothy Buck and Ana G. Lecuona. "Some knots in $S^1 \times S^2$ with lens space surgeries". In: *Comm. Anal. Geom.* 24.3 (2016), pp. 431–470. ISSN: 1019-8385.

[6] Mohan Bhupal and András I. Stipsicz. "Weighted homogeneous singularities and rational homology disk smoothings". In: *Amer. J. Math.* 133.5 (2011), pp. 1259–1297. ISSN: 0002-9327.

[7] Andrew Donald and Brendan Owens. "Concordance groups of links". In: *Algebr. Geom. Topol.* 12.4 (2012), pp. 2069–2093. ISSN: 1472-2747.

[8] S. K. Donaldson. "The orientation of Yang-Mills moduli spaces and 4-manifold topology". In: *Journal of Differential Geometry* 26.3 (1987), pp. 397–428. DOI: 10.4310/jdg/1214441485. URL: https://doi.org/10.4310/jdg/1214441485.

[9] Javier Fernández de Bobadilla, Ignacio Luengo, Alejandro Melle Hernández and Andras Némethi. "Classification of rational unicuspidal projective curves whose singularities have one Puiseux pair". In: *Real and complex singularities*. Trends Math. Birkhäuser, Basel, 2007, pp. 31–45. DOI: 10.1007/978-3-7643-7776-2_4. URL: https://doi-org.ezproxy.lib.gla.ac.uk/10.1007/978-3-7643-7776-2_4.

[10] Marco Golla and Kyle Larson. *3-manifolds that bound no definite 4-manifold*. 2020. DOI: 10.48550/ARXIV.2012.12929. URL: https://arxiv.org/abs/2012.12929.

[11] Robert E. Gompf and András I. Stipsicz. *4-manifolds and Kirby calculus*. Vol. 20. Graduate Studies in Mathematics. American Mathematical Society, Providence, RI, 1999, pp. xvi+558. ISBN: 0-8218-0994-6. DOI: 10.1090/gsm/020. URL: https://doi-org.ezproxy.lib.gla.ac.uk/10.1090/gsm/020.

[12] C. McA. Gordon. "Dehn surgery and satellite knots". In: *Trans. Amer. Math. Soc.* 275.2 (1983), pp. 687–708. ISSN: 0002-9947. DOI: 10.2307/1999046. URL: https://doi-org.ezproxy.lib.gla.ac.uk/10.2307/1999046.

[13] Rob Kirby. "Problems in low-dimensional topology". In: *Geometric topology*. AMS/IP Stud. Adv.Math., vol. 2. Amer. Math. Soc., Providence, R.I., 1997, pp. 35–473.

[14] Ana G. Lecuona. "Complementary legs and rational balls". In: *Michigan Math. J.* 68.3 (2019), pp. 637–649. ISSN: 0026-2285.

[15] Ana G. Lecuona. "On the slice-ribbon conjecture for Montesinos knots". In: *Trans. Amer. Math. Soc.* 364.1 (2012), pp. 233–285. ISSN: 0002-9947.

[16] Paolo Lisca. "Lens spaces, rational balls and the ribbon conjecture". In: *Geom. Topol.* 11 (2007), pp. 429–472. ISSN: 1465-3060. DOI: 10.2140/gt.2007.11.429. URL: https://doi-org.ezproxy.lib.gla.ac.uk/10.2140/gt.2007.11.429.

[17] Paolo Lisca. "Sums of lens spaces bounding rational balls". In: *Algebr. Geom. Topol.* 7 (2007), pp. 2141–2164. ISSN: 1472-2747. DOI: 10.2140/agt.2007.7.2141. URL: https://doi-org.ezproxy.lib.gla.ac.uk/10.2140/agt.2007.7.2141.

[18] Lisa Lokteva. *Surgeries on Iterated Torus Knots Bounding Rational Homology 4-Balls*. 2021. arXiv: 2110.05459 [math.GT].

[19] José María Montesinos. "4-manifolds, 3-fold covering spaces and ribbons". In: *Trans. Amer. Math. Soc.* 245 (1978), pp. 453–467. ISSN: 0002-9947.

[20] Walter D. Neumann. "On bilinear forms represented by trees". In: *Bull. Austral. Math. Soc.* 40.2 (1989), pp. 303–321. ISSN: 0004-9727.

[21] *Online Encyclopedia of Integer Sequences*. https://oeis.org/. Accessed: 2022-02-23.

[22] Oswald Riemenschneider. "Deformationen von Quotientensingularitäten (nach zyklischen Gruppen)". In: *Math. Ann.* 209 (1974), pp. 211–248. ISSN: 0025-5831.

[23] Jonathan Simone. "Classification of torus bundles that bound rational homology circles". In: *arXiv preprint arXiv:2006.14986* (2020).

[24] András I. Stipsicz, Zoltán Szabó and Jonathan Wahl. "Rational blowdowns and smoothings of surface singularities". In: *J. Topol.* 1.2 (2008), pp. 477–517. ISSN: 1753-8416.